

May 2020

## Band Extension and Possible Ridge Compression on Europa

Sarah Chinski

*Macalester College*, [schinski@macalester.edu](mailto:schinski@macalester.edu)

Follow this and additional works at: <https://digitalcommons.macalester.edu/mjpa>



Part of the [Astrophysics and Astronomy Commons](#), and the [Geology Commons](#)

---

### Recommended Citation

Chinski, Sarah (2020) "Band Extension and Possible Ridge Compression on Europa," *Macalester Journal of Physics and Astronomy*: Vol. 8: Iss. 1, Article 5.

Available at: <https://digitalcommons.macalester.edu/mjpa/vol8/iss1/5>

This Honors Project - Open Access is brought to you for free and open access by the Physics and Astronomy Department at DigitalCommons@Macalester College. It has been accepted for inclusion in Macalester Journal of Physics and Astronomy by an authorized editor of DigitalCommons@Macalester College. For more information, please contact [scholarpub@macalester.edu](mailto:scholarpub@macalester.edu).

---

## Band Extension and Possible Ridge Compression on Europa

### Abstract

Jupiter's icy moon Europa has captivated and perplexed the scientific community since the discovery of its global liquid water ocean. Over the course of several missions to the Jovian system, high-resolution observations of Europa have determined that there are spreading zones where new crust is created, similar to the mid-ocean spreading tectonic process we observe on Earth. These features, known as bands, have symmetric hills and valleys, indicating brief events of activity where material from the interior is exuded through a central crack, and solidifies on both sides, creating two positive topography. Recently, European scientists have been questioning how these features affect the total ice volume of the moon. After all, if ice is being created at these features, then the total volume of ice on Europa would be increasing, unless there was some mechanism in place to balance this net positive change in volume.

In this thesis, I begin with a hypothesis: maybe the volume of ice being created through band extension can be compensated by compressional features. To test this hypothesis, we map, measure, and calculate surface area and volume estimates for bands and ridges in four regions across a global mosaic of Europa using moderate resolution images from the Galileo spacecraft. From our results, we may be able to draw important constraints on the thickness of the outer ice shell, which has been highly debated among scientists for decades.

Initial results of this study show that the surface area of ridges can compensate for 35-70% of band surface area, with percentages varying greatly by region. Volume ratios of ridges to bands were calculated for several plausible values of shell thickness, ranging from 100 m - 50 km. It appears that in order to compensate for band spreading, the bands would need to propagate to depths of 200 m – 1 km. While these calculations are only indicative of a small percentage (4.62%) of the total surface area of Europa and therefore are not yet conclusive for understanding the surface expression of tectonic activity, they prompt further investigation on a more global scale.

### Keywords

astrophysics, geology, planetary science, Europa, icy moons, Galileo, Voyager, tectonics

MACALESTER COLLEGE

# Band Extension and Possible Ridge Compression on Europa

by

Sarah Chinski

in the

Department of Physics and Astronomy

Advisors: Moses Milazzo, John Cannon, Anna Williams

May 2020





An artist's rendition of a conceptual Europa lander as it samples the moon's surface, with Jupiter and Io hanging in the sky. Image credit: NASA/JPL-Caltech.

MACALESTER COLLEGE

## *Abstract*

Department of Physics and Astronomy

by Sarah Chinski

Jupiter's icy moon Europa has captivated and perplexed the scientific community since the discovery of its global liquid water ocean. Over the course of several missions to the Jovian system, high-resolution observations of Europa have determined that there are spreading zones where new crust is created, similar to the mid-ocean spreading tectonic process we observe on Earth. These features, known as bands, have symmetric hills and valleys, indicating brief events of activity where material from the interior is exuded through a central crack, and solidifies on both sides, creating two positive topography. Recently, European scientists have been questioning how these features affect the total ice volume of the moon. After all, if ice is being created at these features, then the total volume of ice on Europa would be increasing, unless there was some mechanism in place to balance this net positive change in volume.

On Earth, the change in volume of the crust over time is essentially zero, as the mid-ocean ridge spreading features are compensated by tectonic compression across the globe. When compressed, a rocky crust forms mountains and volcanoes. The results of this tectonic compression is highly dependent on the composition of the crust being compressed. It is still highly debated among European scientists whether the icy crust is brittle or ductile. Brittle ice would compress into a more compact, higher density ice, while a ductile ice may be able to layer ice with less cracking and a lower overall density.

In this thesis, we begin with a hypothesis: maybe the volume of ice being created through band extension can be compensated by compressional features. To test this hypothesis, we map, measure, and calculate surface area and volume estimates

for bands and ridges in four regions across a global mosaic of Europa using moderate resolution images from the Galileo spacecraft. From our results, we may be able to draw important constraints on the thickness of the outer ice shell, which has been highly debated amongst scientists for decades.

Initial results of this study show that the surface area of ridges can compensate for 35-70% of band surface area, with percentages varying greatly by region. Volume ratios of ridges to bands were calculated for several plausible values of shell thickness, ranging from 100 m - 50 km. It appears that in order to compensate for band spreading, the bands would need to propagate to depths of 200 m – 1 km. While these calculations are only indicative of a small percentage (4.62%) of the total surface area of Europa and therefore are not yet conclusive for understanding the surface expression of tectonic activity, they prompt further investigation on a more global scale.

## *Acknowledgements*

This work would not be possible without the guidance and mutual effort of the dedicated individuals who have offered me their unwavering guidance and support.

First, I would like to thank Moses Milazzo for conceptualizing this summer project, and for acting as my go-to Europa Expert. I will treasure your mentorship, your positive attitude and the importance you placed on a work-life balance. You make me want to go to graduate school, get a job at NASA, and eventually become a professor just so I can make one student feel the way you made me feel. You told me to change all of the pronouns from plural (we, our) to singular (I, my), because while others have offered guidance and assistance, this work is my own. You helped me embrace my accomplishments and made this work incredibly fulfilling.

Christian Tai Udovicic was the graduate student who dedicated much of his time and efforts over the summer of 2019 to help me develop the tools and knowledge I would need to complete this research. He was the first person to help me realize I can call myself a European scientist. Thank you Christian, for acting as the graduate student and mentorship role-model I needed. I can only hope to live up to the standards you've shown me.

Thanks to John Cannon, my academic advisor for four years, who gave me my first research opportunities and allowed me to participate in research and coauthor two previous publications. By the end of our first-year course *Exosolar Planets and Astrobiology*, I knew that studying icy moons was going to be my dream career. You have provided necessary commentary on countless papers that have improved my capabilities as a writer, and your intense academic rigor has made me a better student. I have always wanted to make you proud.

Thanks to Anna Williams for acting as a member of my defense committee, and helping me early on with time-management advice for a project I knew was going to require a lot of advanced planning. Thanks to Jim Doyle for submitting almost 20 letters of recommendation on my behalf to summer programs, including for my application to NAU.

I would like to thank my partner, Joey Undis, for his help troubleshooting countless Latex formatting errors and broken Excel formulas. You have helped polish this work and make it something I can be proud of, and your emotional support has been invaluable during what has been the most challenging yet rewarding experience of my academic career.

Finally, I would like to thank Christopher Edwards for allowing me to work in his lab all summer, and David Trilling for his guidance and leadership as the head of our REU cohort. Thanks to all of my friends from the summer of 2019 at NAU: my roommates Hana Sun and Lauren Tafla for laughter, inspiration, and for making my summer shine, and to Alexander Kling, Ben Wing, Cheyenne West, Cody Huls, Colin Murphy, Giannina Guzman, Katherine Lutz, Patrick Behr, and Victoria Leger for all the adventures.

Special thanks to the National Science Foundation (NSF) for providing the grants that allowed all of us to pursue our passion projects, and to Northern Arizona University Physics and Astronomy department for providing the facilities for all of us to work, as well as educational opportunities and field trips to geological sites to enrich our experience.

Cheers to us, to clear skies and to long nights.

*Sarah Chinski*

# Contents

---

<b>Abstract</b>	<b>iv</b>
<b>Acknowledgements</b>	<b>vi</b>
<b>1 Introduction</b>	<b>1</b>
<b>2 Background</b>	<b>6</b>
2.1 Past Missions . . . . .	6
2.2 Orbital Mechanics . . . . .	9
2.3 Subsurface Ocean . . . . .	11
2.4 Tectonics . . . . .	13
2.5 Surface Geology . . . . .	21
<b>3 Mapping Techniques and Calculations</b>	<b>31</b>
3.1 Mapping Overview . . . . .	31
3.2 Classification of Surface Features . . . . .	34
3.2.1 Ridge Classification . . . . .	34
3.2.2 Band Classification . . . . .	37
3.3 Models for Calculation . . . . .	38
3.3.1 Bands . . . . .	38
3.3.2 Height from Shadow Length . . . . .	39
3.3.3 Triangular Ridges . . . . .	40
3.3.4 Rectangular Ridges . . . . .	41
3.3.5 Elliptical Ridges . . . . .	41
3.3.6 Rectangular wedge . . . . .	42
3.3.7 Triangular wedge . . . . .	42
<b>4 Data Analysis</b>	<b>43</b>
<b>5 Results and Discussion</b>	<b>47</b>
<b>6 Error Analysis</b>	<b>52</b>
<b>7 Future Missions</b>	<b>53</b>
7.1 Europa Clipper . . . . .	53
7.2 JUICE . . . . .	54

<i>Contents</i>	ix
<b>8 Conclusion and Future Work</b>	<b>55</b>
<b>A Mapping Techniques</b>	<b>57</b>
<b>Bibliography</b>	<b>59</b>



## CHAPTER 1: Introduction

---

In 1979, NASA's two Voyager spacecraft sped past the moon and saw a surface littered with scars and cracks— and, most importantly, evidence for an extensive liquid water ocean beneath an icy crust (Pappalardo et al. (1999)). Voyager inspired numerous missions to the Jovian system, and Europa became a high-priority target. More recent missions have shown an immensely chaotic surface, which has since been categorized into five broad components shown in Figure 1.1: plains, chaos terrain, craters, ridges, and bands (Greeley et al. (2000)).

The plains, or “background matrix”, is the oldest material on the surface of Europa, and appears to be a series of overlain, faded ridges and bands. On the other hand, chaos terrain is often some of the youngest material on Europa, and have had dozens of complex mechanisms of formation proposed since their discovery (e.g., Pappalardo et al. (1999), Schmidt et al. (2011)). In general, chaos terrain is thought to form when thermal plumes travel outwards from the interior, which melt and warp the surface (Schmidt et al. (2011)). While chaos terrain is quite common, craters are more difficult to locate. The general lack of impact craters was the first indication of the young surface age, as crater counting is one of the simplest methods of age-dating methods astronomers use to approximate the age of the surface of a solar system body (Bierhaus et al. (2005)). There must be an active mechanism at play to recycle the surface content and eliminate craters. Based on the low spatial density of craters on Europa, it is estimated that the surface is only 60-90 million years old (Leonard et al. (2018)). For comparison, the oldest rocks on Earth's surface are over 4 billion years old, and oceanic crust age is typically around 125 million years old (Müller et al. (2008)).

In this work, we focus on the two remaining surface features: bands and ridges. Drawing connections between the two could provide valuable insight into the active surface processes. Bands are the more well-understood than ridges, and can be most simply described as extensional features where new crust is created, similar to how mid-ocean ridge spreading zones form on Earth. Based on the symmetry of these features (see Figure 1.2), the general consensus is that bands form as material from the interior is incrementally ejected through a break in the surface, then

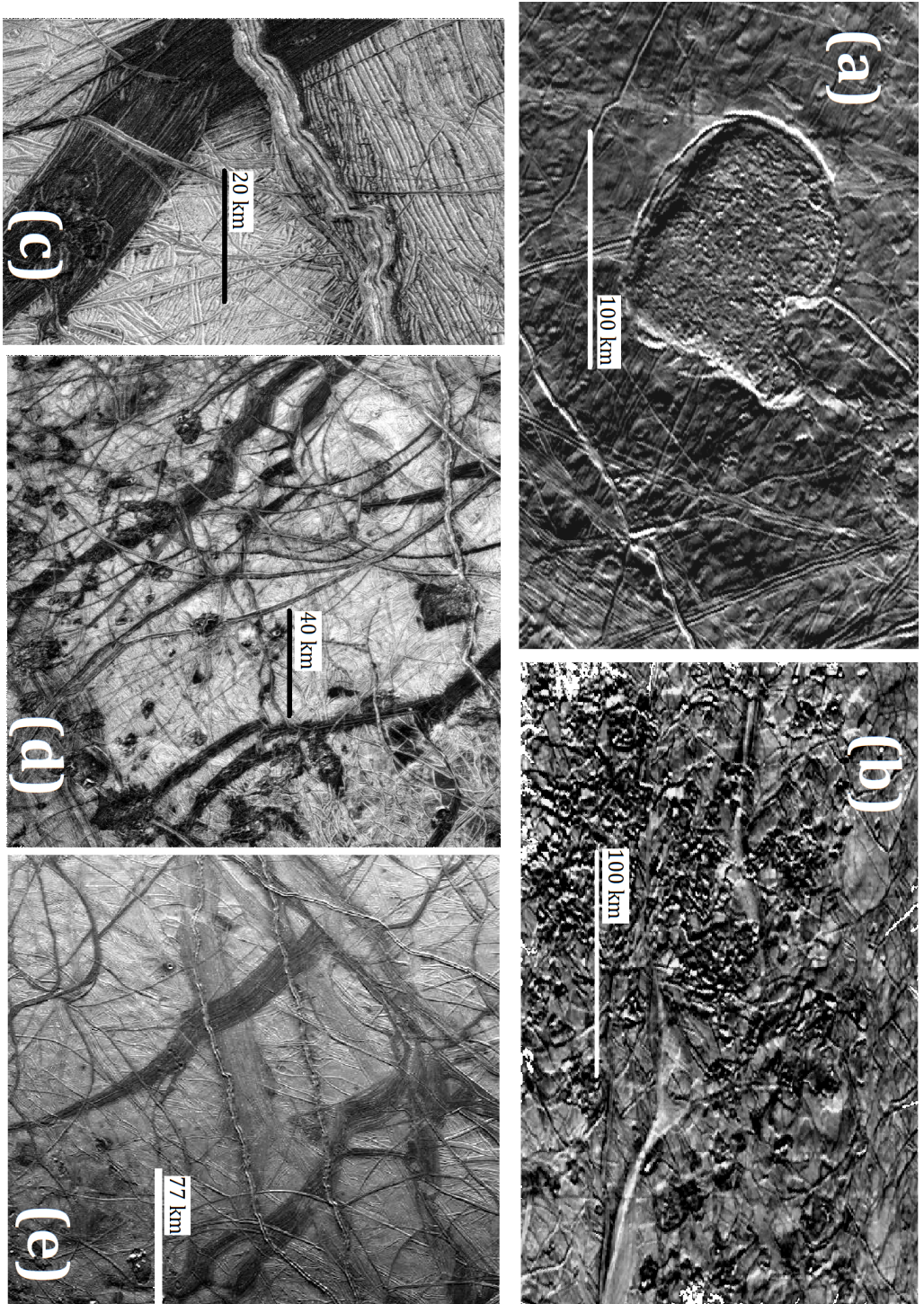


FIGURE 1.1: A variety of surface features were observed across the four sites selected for this study. (a) and (b) show two types of chaos terrain, and based on the law of superposition the youngest material lies on top of older material. The mitten-shaped chaos terrain in (a) is relatively smooth in comparison to the surface of (b), which is rough and hummocky with many boulder-shaped clusters. (c) shows a high-resolution image of a ridge (bright, central and near-horizontal feature) overtop a band (dark feature in the lower left). (d) shows a variety of bands, ridges, the background plains, and various chaos terrain features (including the dark domes/pits known as lenticulae). (e) encompasses all of Site 1 with all 5 types of surface terrain visible.

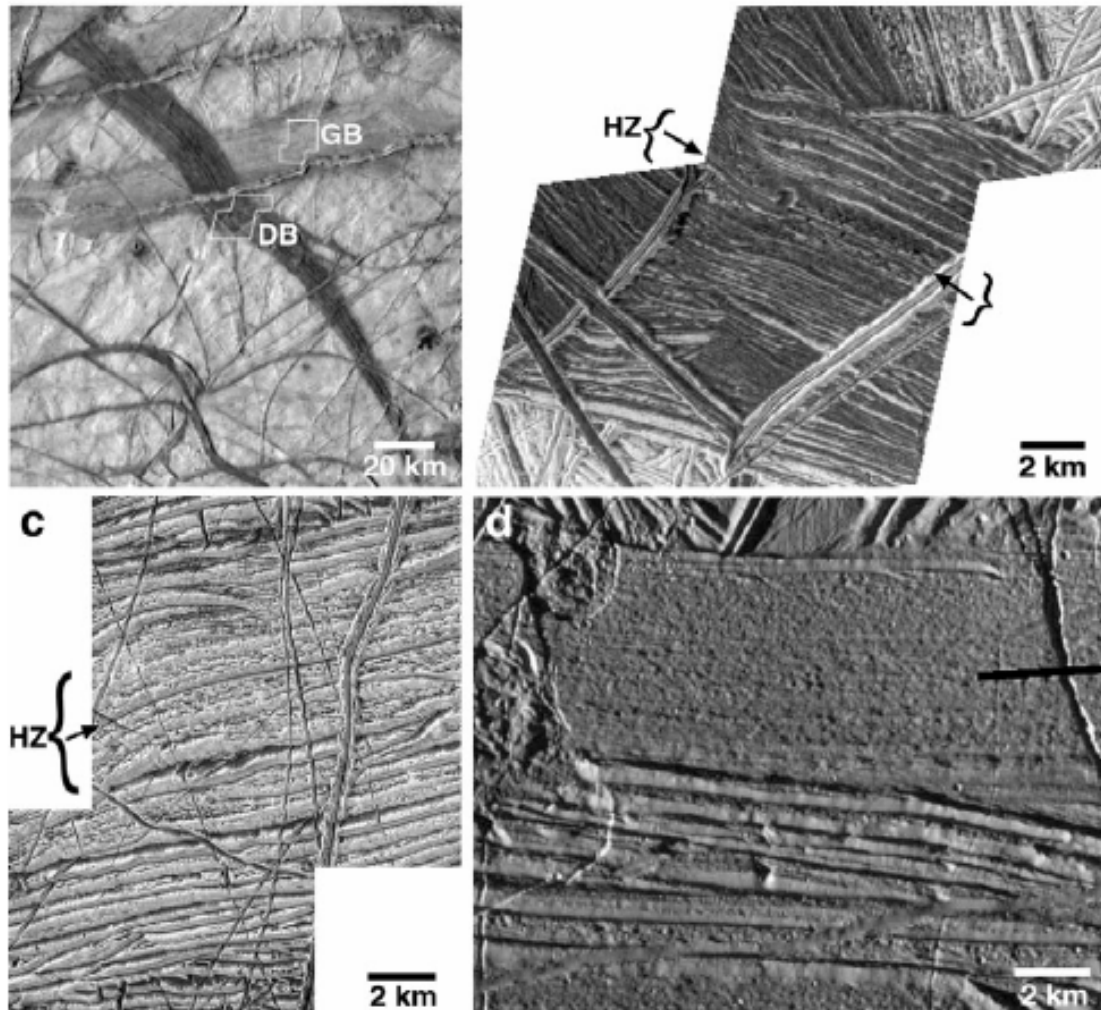


FIGURE 1.2: Image and caption from [Pappalardo \(2010\)](#): Examples of bands on Europa. (a) A dark wedge-shaped dark band (DB) cross-cuts a brighter (older) gray band (GB). (b) At high-resolution, the dark band shows multiple subparallel ridges and troughs that flank a central trough (arrows) and hummocky zone (braces, HZ). (c) At high resolution, the gray band shows similar characteristics of a central trough (arrow) and hummocky zone (braces, HZ). (d) A band seen at high resolution and high solar incidence angle displays subparallel ridge and troughs with characteristics of normal fault blocks. These characteristics have been compared to spreading centers on Earth.

solidifies ([Stempel et al. \(2005\)](#)). Ridges are high-albedo features with positive topography and height estimates on the order of several hundred meters, and lengths from several hundred meters to thousands of kilometers ([Leonard et al. \(2018\)](#)). A high-resolution image of many overlapping ridges is shown in [Figure 1.3](#).

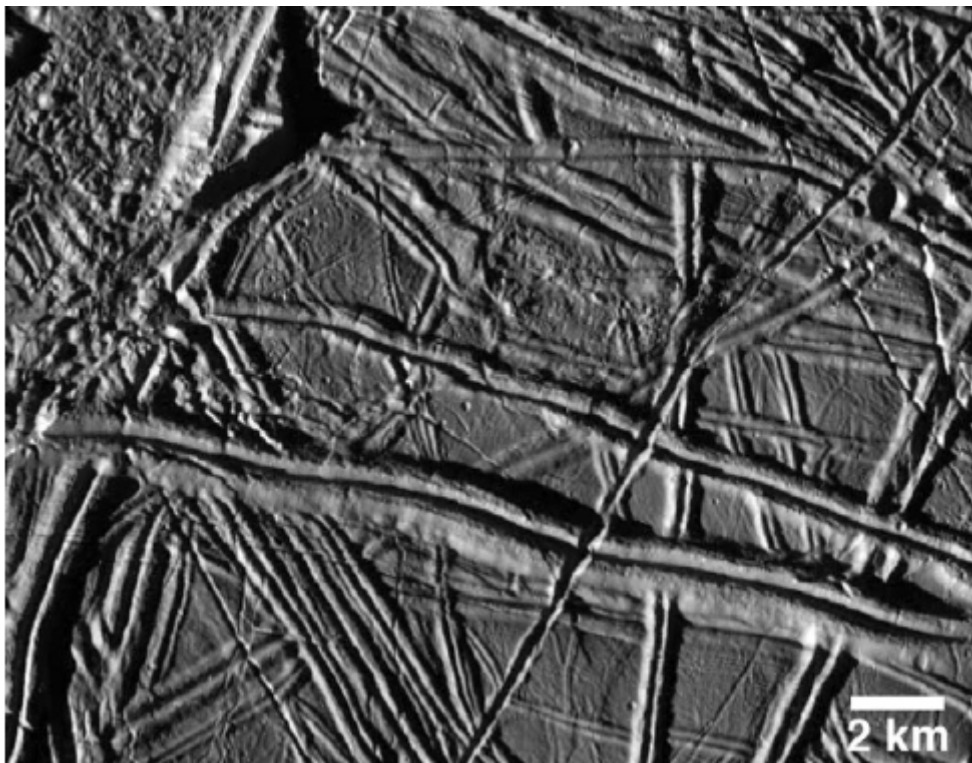


FIGURE 1.3: Figure from [Pappalardo \(2010\)](#): A high resolution image containing many double ridges (younger) overlaying multi-ridge complexes (older), and possible chaos terrain in the upper left interrupting a near vertical double ridge. Ridges have heights estimated from tens to hundreds of meters and can propagate for thousands of kilometers ([Leonard et al. \(2018\)](#)).

While there is a general consensus on the nature of band formation, the processes surrounding ridge formation are still debated. Some theories predict ridges may form via cryovolcanism, where material is ejected around a central crack to create the positive topography we observe ([Geissler et al. \(1998\)](#), [Head et al. \(1999\)](#), [Greenberg et al. \(1998\)](#)). If, however, ridges act as the compressional counterpart to the extensional bands, similar to convergent plate boundaries on Earth, then the volume ice created at bands could be compensated by the compressional ridges, where ice could be compacted or destroyed. To test this hypothesis, we have mapped ridges and bands across three locations on Europa, and calculated surface areas and estimated volumes for several geometric models of these features. If the volume estimates for bands and ridges are within 1-2 orders of magnitude of each other, it is possible that ridge compression can compensate for band expansion, as these values would lie within error bounds of the calculations. However, if the new surface being generated through band expansion greatly exceeds ridge volume

by several orders of magnitude, this does not lie within error of our results and therefore there must be some other mechanism that is removing the ice being created at bands (or the radius of Europa would be increasing).

## CHAPTER 2: Background

---

### 2.1 Past Missions

#### Voyager

The twin spacecraft Voyager 1 and 2 arrived at Europa in 1979. While Voyager 1 was too far from the moon to make out many surface details, Voyager 2 was able to capture images which revealed a lively and enigmatic surface (See Figure 2.1). These images showed fragmented plates of ice on an unusually young surface, which were major lines of evidence in favor of a tectonically active surface. From this data, European scientists could begin to classify large-scale landforms such as bands and ridges, which were made visible for the first time at resolutions up to 2 km/pixel. These discoveries laid the foundation for what future missions would eventually explore.

#### Galileo

Following the successes of Voyager 1 and 2, the Galileo spacecraft was the fifth mission to enter the Jovian system (two Pioneer spacecraft preceded Voyager 1 and 2, but obtained few notable images). Galileo was unique in that it was the first to enter into orbit around the planet, as data collection from previous missions were severely limited by the singular flyby. With a decade of technological advances between the launch of Voyager and Galileo, the science team wanted the resolution and quantity of the data from this mission to far exceed its predecessors capabilities.

Thus, Galileo came equipped with ten scientific instruments. Some of the non-camera instrumentation includes two plasma detectors to detect low charged particles and electromagnetic waves, a high-energy particle detector, and an ultraviolet detector and spectrometer. Many of these helped identify chemical composition of the surface, although attempts at mapping observed spectrometer data with images have been unsuccessful, likely due to the low resolution capabilities of spectrometers at the time. The camera system included a Near-Infrared Mapping



FIGURE 2.1: Voyager 2 captured Europa's striking surface features. The dark scars on the surface are bands, while large ridge systems also seem visible as a thin white stripe through the center of a long and dark band-like features. Rounded domes or pits (called lenticulae) are visible as dark splotches, and the poles are heavily scarred by thin and ridges. Image credit: NASA/JPL/Ted Stryk

Spectrometer (NIMS), which produced multispectral images of the atmosphere and surface for chemical analysis.

With the influx of new data from Galileo, our knowledge of Europa's exterior has greatly expanded. Many theories began to develop to explain the features observed at the mid- to high-resolution images. For example, NIMS revealed the presence of hydrated minerals on Europa's surface. These minerals have been interpreted as hydrated magnesium and sodium salts and sulfates (Quick & Marsh (2016)). While these components have been cited as evidence for a highly acidic or salty ocean (Kargel et al. (2000) and Pasek & Greenberg (2012)), the exact oceanic composition remains elusive.

Even with several intricate missions, Europa keeps some secrets. One important detail which has eluded scientists has been the exact thickness of its icy outer shell. While gravitational and magnetometer data have revealed the presence of a global liquid water ocean, the thickness of that ocean and the over laying ice shell are unknown. From our current data, there is no way of directly measuring the ice shell thickness, though this missing piece has inspired remarkable creativity and innovation from those studying Europa. For decades, attempts have been made to model the formation and evolution of observed surface features in hopes that analysis of these features could provide important constraints on the range of values for the ice shell and ocean thickness, which is the broadest goal of this thesis.

## Hubble

The Hubble Space Telescope (HST) has proven itself capable of viewing one of the most important processes on Europa to date. Roth et al. (2013) discuss the discovery of plumes of water vapor ejected into the moon's atmosphere, similar to those famous plumes from the tiger stripes of Saturn's moon Enceladus. These detections could not have been made by the Galileo spacecraft, as the surface area of the fractures which allow plume ejecta are too small to produce a thermal anomaly that would be detectable by Galileo's instrumentation.

The authors match HST observations with Galileo data at its closest approach (>400 km altitude) where the Plasma Wave Spectrometer detected a brief but substantial increase in plasma density, which would match the signal created by a

plume matching HST's observed characteristics ([Jia et al. \(2018\)](#)). This provides continued evidence for plumes on Europa, but are not yet indicative of plumes being a common or global occurrence. While few advancements in our understanding have been made at the conclusion of Galileo's mission, HST has been able to successfully supplement past observations in the time between dedicated missions to Europa. Future mission prospects will be discussed in Chapter 7.

## 2.2 Orbital Mechanics

The three Jovian moons Io, Europa, and Ganymede have one of the most famous and unique configurations in the solar system. The moons are locked in a 1:2:4 orbital resonance called a Laplacian resonance ([Peale & Lee \(2002\)](#), see [Figure 2.2](#)), meaning Europa's orbit is twice as long as Io's, and Ganymede's orbit is four times as long as Io's and twice as long as Europa's. This orbital configuration is stable and self-correcting, and leads to a number of periodic configurations where successive conjunctions lead to strong tidal interactions along the same surface feature ([Ogihara & Ida \(2012\)](#)).

The specifics of these orbital patterns create interesting implications for the surface features observed on Europa, particularly the ridges. Some ridges have a cycloidal appearance (see [Figure 2.3](#), and it's been theorized these features form as a result of tension cracks during diurnal tidal variations in combination with Europa's slightly eccentric orbit ([Hoppa et al. \(1999\)](#)). During close approach to Jupiter, Ganymede, or Io, tidal forces can overcome the tensile strength of the ice at weak points in the crust, and will propagate as the direction and strength of tidal stresses change during orbit. After closest approach, the tidal stress will decrease until it reaches the tensile ice strength and the cycloidal crack will cease propagation.

It was only recently discovered that Europa's orbit is not a perfect circle (its eccentricity is not zero), but it has a forced eccentricity caused by the gravitational orbital resonances between Europa, Io and Ganymede ([Greenberg et al. \(1998\)](#)). Europa's minor eccentricity is enough to create a variation in stress on the surface that's dependent on the orbital configuration. This eccentricity, along with the

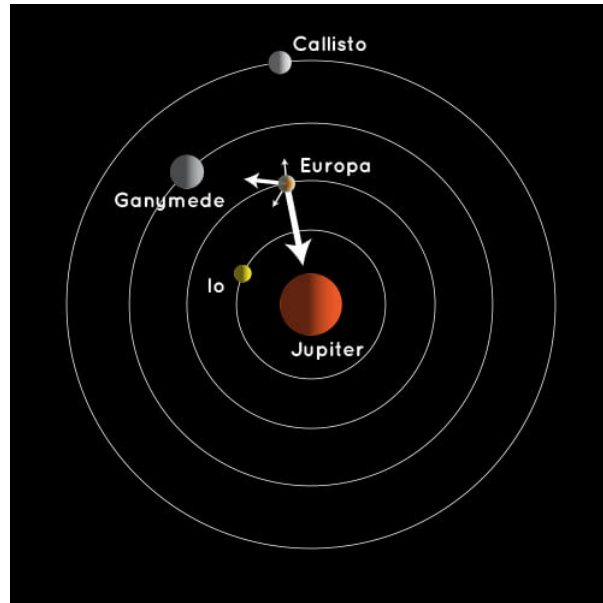


FIGURE 2.2: Shows the relative magnitude and direction of the gravitational forces acting on Europa. While all four Galilean moons are featured, Jupiter, Ganymede and Io have the greatest gravitational influence on Europa.  
Image credit: NASA

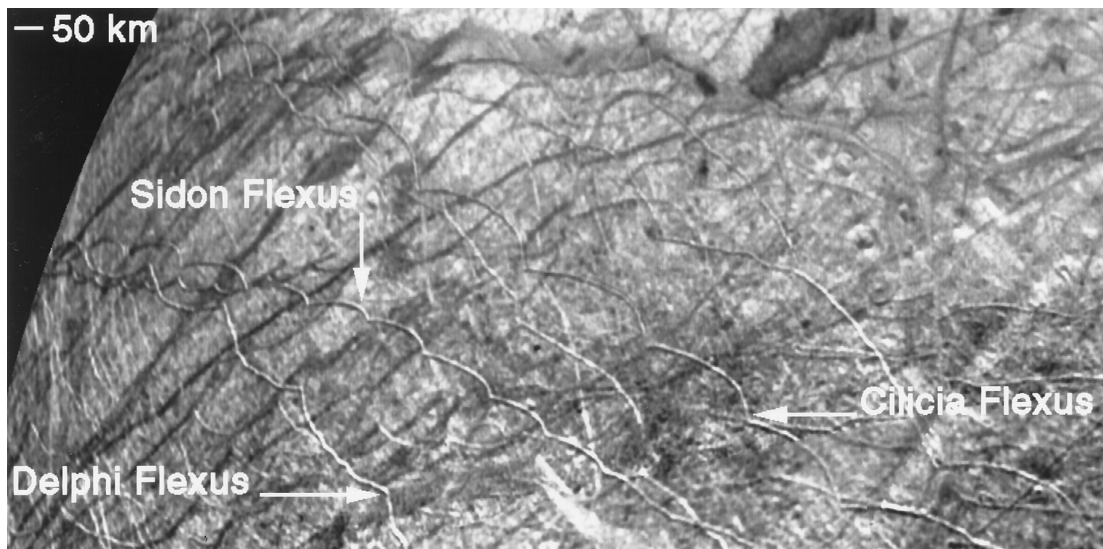


FIGURE 2.3: Figure from [Hoppa et al. \(1999\)](#): pictured are the many cycloidal features, which have a positive topography and heavily populate the north and south poles. A cycloid is mathematically defined as the line traced by the point on a circle as it rolls in a straight line. These unusual features have been hypothesized to form due to orbital stresses acting on a pre-existing crack or weakness in the crust.

Laplacian resonance, are the major factors attributed with creating these strange patterns of cycloidal ridges.

The stress fields caused by the the orbital resonances and forced eccentricity could explain a variety of features on Europa across a range of latitudes, as a modest change in magnitude ( $\sim 8$  kPa according to [Hoppa et al. \(1999\)](#)) and propagation speed could produce the cycloids. A variation in force across the surface could be explained by variable plate thickness, which is not ruled out in current models of Europa. Often times a uniform plate thickness is assumed for simplicity, though some models portraying the interior of Europa depict an variable plate thickness.

## 2.3 Subsurface Ocean

Through data analysis of surface geology, orbital mechanics, and magnetic field of Europa planetary scientists have been able to produce a theoretical model of Europa's interior. Europa has a bulk density of  $3.01 \text{ g/cm}^3$  which is close to the density of Earth's moon and suggestive of a rock-dominated composition ([Showman & Malhotra \(1999\)](#)). While most of the interior may be molten rock, the magnetic fields detected by Galileo suggest the existence of a layer of liquid beneath the icy surface ([Kivelson et al. \(1999\)](#)).

The existence of a subsurface ocean is necessary to explain nearly all of Europa's surface features. A typical model of Europa depicts an icy outer shell encasing a subsurface liquid ocean, which are both overtop a thicker rocky shell surrounding an iron core ([Greeley et al. \(1998\)](#), [Hall et al. \(1995\)](#)). The thickness of these layers is debated, but a general model is provided in [Figure 2.4](#). It is unclear whether this ocean is decoupled from the outer ice shell, although some planetary scientists argue the rates of motion of the crust is indicative of a decoupled outer shell ([Gaidos & Nimmo \(2000\)](#)). A mechanical coupling would function similarly to the crust-mantle coupling on Earth, as the motion of the crust is directly linked to the convectational motion of the upper mantle, the asthenosphere. On the other hand, a decoupled ocean would allow for greater tidal force effects from Jupiter to act on the independent surface, and possibly allow for faster movement of the ice shell than subsurface convection could provide.

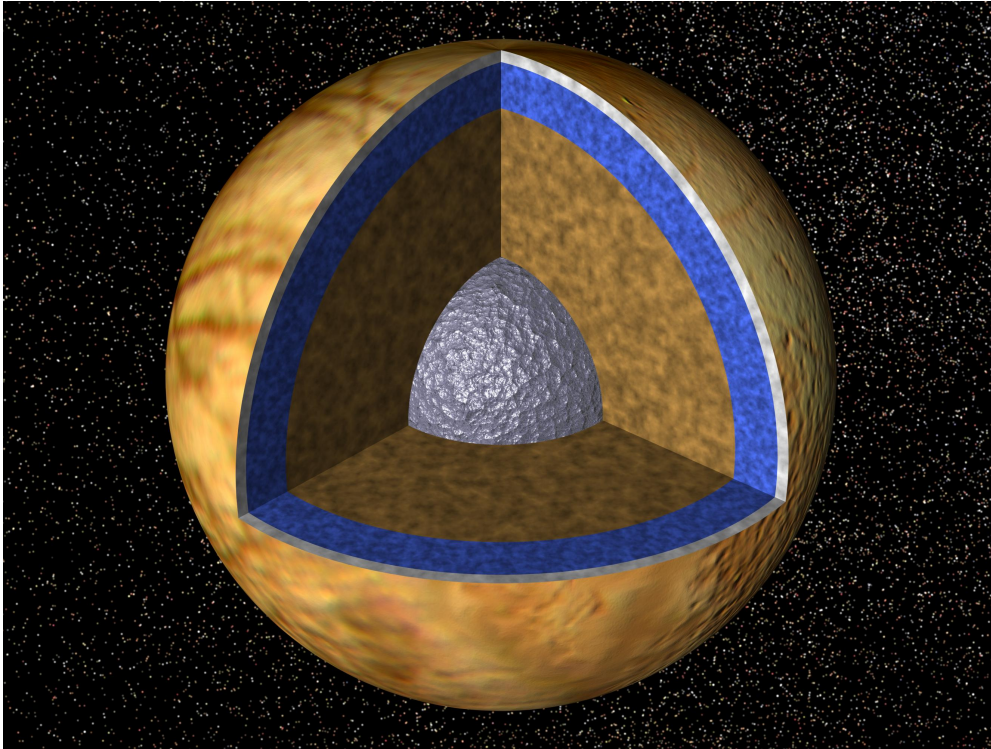


FIGURE 2.4: A plausible cross-section of the interior structure of Europa. The surface topography is a mosaic of Voyager 1 images. The interior characteristics are inferred from Galileo gravitational and magnetometer data. Pictured is a metallic iron core (gray) surrounded by a thick rocky shell (brown). The blue and white layers represent the shell of liquid water ocean and icy crust, which are each of highly debated thickness. Image credit: *NASA/JPL*.

The existence of a subsurface liquid ocean is a necessary component to explain the observed tectonic features on the surface. In the case where Europa has active tectonics modeled similarly to Earth's tectonics, the observed surface features would be formed through the motion of the ocean driving the movement of the fractured surface plates. Band spreading, which may function similarly to midocean spreading zones on Earth, are among the most well modeled active processes. However, for the volume of the outer ice shell to be constant (and thus the radius of Europa not to be increasing), the ice created in these zones must be balanced by a process acting to eliminate surface ice elsewhere. In this work, I explore the possibility that the ice created at extensional features such as bands could be destroyed or compacted through ice compression at ridges.

## 2.4 Tectonics

Having a basic understanding of orbital mechanics and the subsurface ocean of Europa allows us to begin to explore active tectonics. The gravitational tidal forces and ice shell floating on a liquid ocean are two main mechanisms in our understanding of active tectonics on Europa, and they both have major influences over the types of surface features we see today. Importantly, a detailed understanding of tectonic processes is necessary for the analysis presented later in this study. While there is not currently enough high-resolution coverage from Galileo to produce a global tectonic model of Europa, some research has used Galileo imagery to create localized regional tectonic models of the surface (e.g., [Rhoden et al. \(2012\)](#) and [Kattenhorn & Prockter \(2014\)](#)). There have been hundreds of publications regarding Europa's tectonics, and this section will explore some of the most detailed and intricate among them.

In this section, it is important to note that many of the studies discussed propose models and theories to explain the observed surface features, but that does not necessarily mean that each model proves the existence of their proposed mechanism. While some general models have assumed to be correct based on the mounting evidence in favor of them (for example, the existence of strike-slip faults), the more intricate details of these models are less certain. Many rely on interior mechanics which at current time cannot be tested, only hypothesized.

### Faults and Ice Behavior

Geological faults were some of the first tectonic features observed on Europa's surface. [Rhoden et al. \(2012\)](#) analyze the energy and movement associated with strike-slip faults, a type of fault where plates are not pushed up or down but slide against each other horizontally (See [Figure 2.5](#)). The authors include several key factors which were not included in past, more simplistic models: elastic rebound, stress relaxation over time, a failure threshold, and cumulative shear stresses. These factors add complexity, making their model more robust and realistic. Elastic rebound refers to the assumption that the icy shell has elastic qualities, allowing it to stretch and not necessarily break over small and short

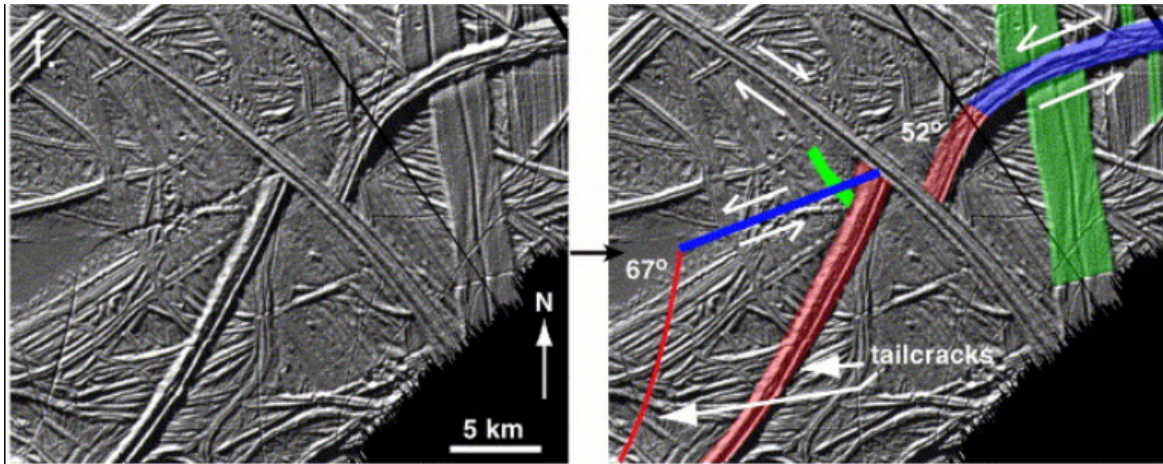


FIGURE 2.5: Figure from [Kattenhorn \(2004\)](#): Some strike-slip fault movements on Europa, with arrows indicating relative motion. In this image, older ridges have been broken and shifted horizontally by another intersecting ridge.

tidal fluctuations. This assumption would lead to significantly fewer surface fractures as a result from periodic resonance interactions between Europa, Ganymede, and Io. Similarly, shell relaxation accounts for the observed viscosity of the outer ice shell. By incorporating a small relaxation factor in their model, [Rhoden et al. \(2012\)](#) are able to model the ice's capabilities to relax at compressional features, which results in a significant net offset in fault movement over time compared to models which do not account for shell relaxation.

Inclusion of a failure threshold means that a horizontal fault will slip and release its stored potential energy at a defined shear stress threshold. This threshold is determined by the volume of the ice and its ability to store potential energy, and can be defined as the force required to fracture the ice. It also allows for the possibility of large-scale earth/ice-quake events during maximum tidal extension and/or compression. Finally, accumulated shear stress should be considered in addition to tidal shear stresses from previous models. In an active tectonic system, ice is able to store stress as potential energy, and the amount of stored stress is referred to as the accumulated shear stress. A model with ductile ice is able to store more energy than brittle ice, as the ductile ice is able to bend/flex to allow for the storage of energy. A brittle ice has less energy storage capabilities and will crack or break to release energy. This stored stress factor adds new and realistic dimension to previous tectonic models, as plates can undergo motion and tectonic processes

outside of peak maxima and minima tidal forces. These factors in combination may explain why some ridges do not align with observed tidal stresses. However, it is still unknown whether the ice is brittle or ductile, as arguments have been made for both cases ([Kattenhorn & Prockter \(2014\)](#)). It is possible that the shell could be fragmented into brittle and ductile layers, or that there are localized locations of ductile ice among a mostly brittle surface.

Thickness and physical properties of the icy crust have also been inferred based on observations of the surface morphology, the induced magnetic field, tidal dissipation, and orbital evolution ([Klaser et al. \(2018\)](#)). Researching each of these components shows a variety of results, and they can be classified into two categories of models. The first model depicts a thin and brittle but conductive ice layer with thickness estimates ranging from 0.1 km to 8 km. This value is based on mechanical models, and does not rule out the possibility of this thin layer overlying a thicker layer of ductile ice. Evidence for a thin icy crust overlying an ocean relies on chaos terrain that look like irregular tabular blocks of ice seem to have floated and drifted over a liquid sea, suggesting a crust thickness of one or two kilometers. The second model type is a thick and entirely solid ice crust with thickness ranging from 2.1 km to 40 km. This model is based on thermal analyses, thermal equilibrium and temperature gradient calculations, and imply the existence of a ductile, convecting layer of warm ice beneath the brittle surface layer. The brittle layer could range in thickness from 0.1 km to 6 km, and the warm, ductile ice layer from 2 to 34 km.

Overall, studies of tectonic faults where motion of plates is observed have produced many hypotheses about the behavior of the ice, on both a global and local scale. The two most commonly referenced models for the outer ice shell can be sorted into two categories: thick and ductile or thin and brittle. Unfortunately, this means we currently don't understand the behavior of ice on the surface, which limits our analysis as discussed later in [Chapter 5](#).

## **Subduction**

Another recent study of the surface geology of Europa takes a different approach than [Rhoden et al. \(2012\)](#). [Kattenhorn & Prockter \(2014\)](#) created a geological reconstruction of one region based on Galileo imagery to model the tectonic processes

of the outer shell. Using this model, they identified plate boundaries observed on Earth: convergent subduction zones, divergent spreading zones where new ice is created (bands), and even strike-slip horizontal faults (see Figure 2.5). The authors define subduction as the downward movement of the portion of a surface below an adjacent plate. Buoyancy would prevent the plate from moving directly into the ocean, and confines it to the warm convecting layer where it is ultimately destroyed. They estimate that the density difference between the underlying warm convecting ice and the top brittle layer is sufficient for subduction to occur.

As we cannot physically observe an interior process which could be driving this motion, [Kattenhorn & Prockter \(2014\)](#) created cross-sectional conceptual models for these different plate boundaries. An example model of subduction is provided in Figure 2.6. Their model predicts a two-part shell with a thin and brittle outer ice layer overtop a thick convecting ice layer, where active ice plate tectonics can recycle the surface material effectively. The thicker convecting ice may act like the asthenosphere, the upper part of the mantle on Earth which is nearly solid but still experiences convection. It is important to remember that while this model can explain observed features (cryolavas and lenticulae, some ridge complexes), it is only one of the possible explanations for the observed surface features and does not prove that there is active subduction on the surface.

Another major component of their study involved creating a tectonic reconstruction ice plates based on the misalignment of geologic features. At some plate boundaries, features that cross the fault are offset, which is evidence of lateral and divergent motion of plates. This is similar to the evidence presented for strike-slip faults, although there would be vertical component in addition to the horizontal (lateral) motion. With their tectonic reconstruction, they found 15% of surface area attributed to subduction (and therefore compression) could accommodate some of the 10-40% observed new surface area created through band formation. This is not ideal when considering our initial hypothesis, as we would expect subduction to accommodate for the majority of the area created through band extension. Based on their results, compression itself would not be able to compensate for all the ice created at bands. I will compare these values to our calculated values in the Analysis section (Chapter 5).

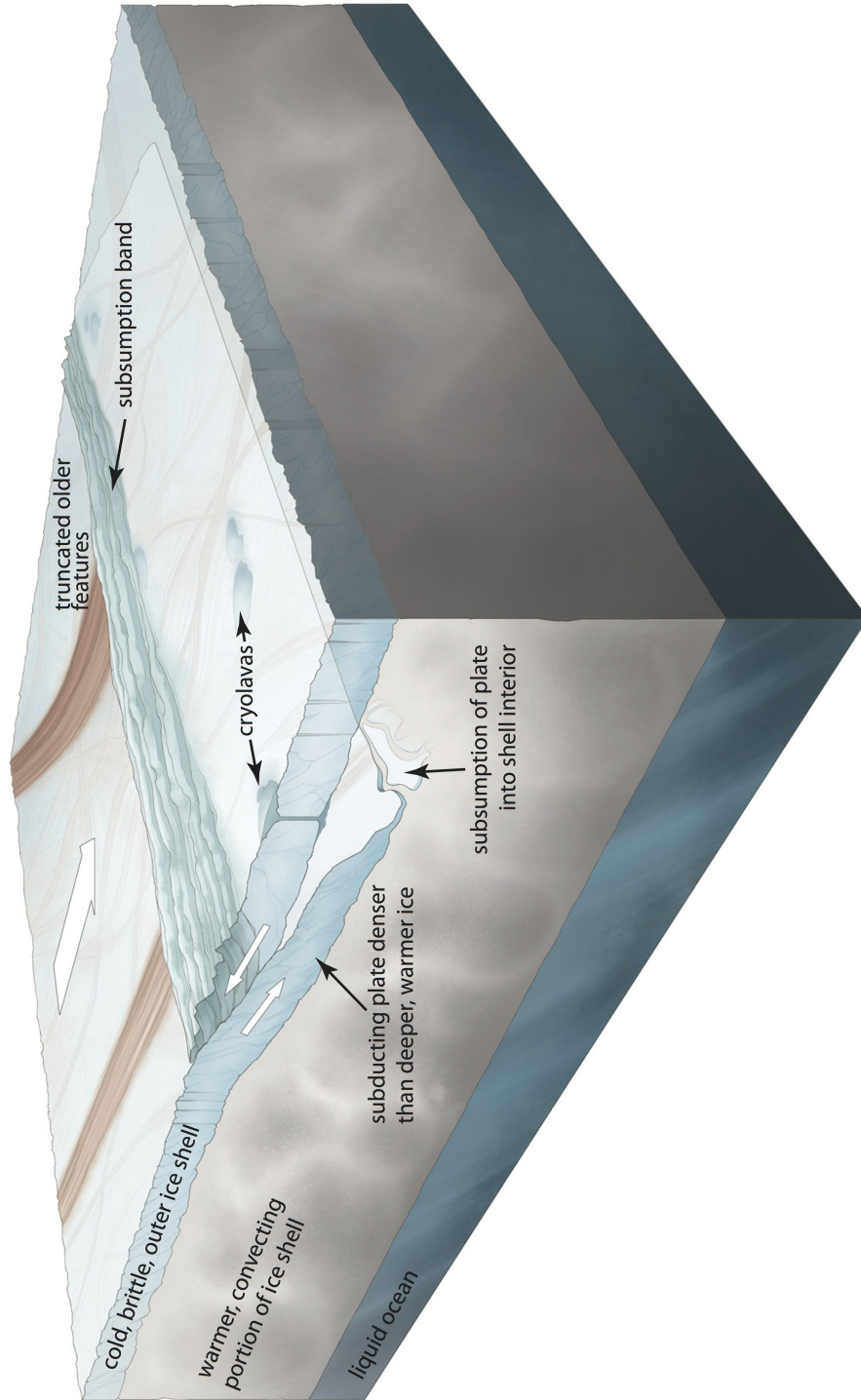


FIGURE 2.6: Figure from [Kattenhorn & Prockter \(2014\)](#): A conceptual model for subduction. The cold, brittle, and more dense outer portion of the ice shell is tectonically pushed into the warmer interior, where it melts and creates thermal plumes of cryolava (the pits/domes also known as lenticulae) that bubble upwards to the surface. This model is conceptually similar to convergent plate boundaries on Earth and the formation of volcanoes, as warmer pockets of molten rock initiate volcanism at convergent (mountain-building) plate boundaries. Plate collision results in crumpling adjacent to the collisional margin, creating band-like structures with parallel hills and troughs.

An earlier study by [Hoppa et al. \(1999\)](#) found that the force required to initiate subduction processes needs to reach magnitudes of 25 MPa is required to form cracks, and 15 MPa is necessary to continue the propagation of the initial crack. [Klaser et al. \(2018\)](#) found two mechanisms which could create forces of this magnitude: non-synchronous rotation and true polar wander. True polar wander is a phenomena most simply described as a change in the geographic locations of the north and south pole due to a “wobble” of the body’s axis of rotation. This phenomena is usually caused by natural inconsistencies in density within the planetary body, as the orientation of the body will attempt to align the maximum moment of inertia with the axis of rotation.

Synchronous orbits occurs in many planet-moon systems, when the rotation of the orbiting body slows and eventually synchronizes with the body it is orbiting. When the moon completes one full revolution for each full orbit, it becomes tidally locked where the same face of the moon stays visible to the planet. Some nonsynchronous rotation has been predicted for Europa, where the outer icy shell and the interior rotate at different rates. This decoupling could be accomplished by a liquid layer separating the ice from the rocky mantle. A diagram of these changing tidal forces is provided in [Figure 2.7](#). Together, these polar wander and nonsynchronous rotation could create variation in forces on the order of several MPa, enough to drive plate subduction.

[Gaidos & Nimmo \(2000\)](#) suggest that larger strike-slip motion may act in a similar fashion to transform plate boundaries on Earth, building up potential energy before a rapid displacement causes a release of that potential energy as mechanical energy; an icy earthquake. While the subject of cryoseismology is still under the early stages of development and research ([Podolskiy & Walter \(2016\)](#)), the claims that [Gaidos & Nimmo \(2000\)](#) make are not unreasonable. They suggest these larger scale energy release events may lead to partial melting along the faults as energy is released as heat, rather than as the destructive earthquake mechanical energy we are accustomed to on Earth.

However, this model also requires a liquid ocean which is mechanically coupled to the crust to allow for a significant tectonic motion to account for observed surface features. This mechanical coupling is assumed to function similarly to

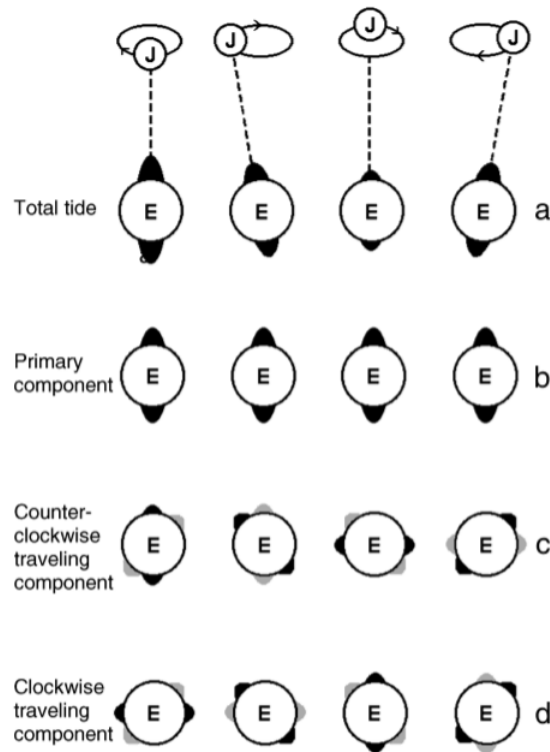


FIGURE 2.7: (Figure and caption (modified) from [Greenberg et al. \(1998\)](#)): A model showing the diurnal tides on Europa throughout its orbit: (a) shows the epicyclic motion of Jupiter over one orbital period, where the tidal force is greatest at pericenter on the left. (b) Shows the primary component of the tidal force, which has constant magnitude and is aligned with the mean direction of Jupiter. If Europa experiences synchronous rotation, this primary component produces no tidal stress, but if Europa rotates nonsynchronously, the primary component will create significant tidal stress described by the one clockwise and one counter clockwise component shown in (c) and (d). These fluctuations are caused by polar wander and the forced eccentricity in Europa's orbit due to its Laplacian resonance. Polar wander involves the wobble of a planet or moon on its axis of rotation, which exposes different regions to tidal flexure based on the orbital configuration. The forced eccentricity allows for nonsynchronous rotation, as the torque exerted by Jupiter can allow the ice shell to rotate faster than the core of the moon. Therefore, the outer ice shell could be decoupled by the liquid layer, and Europa may exhibit nonsynchronous rotation.

the crust-mantle coupling on Earth, as the motion of the crust is directly linked to the convectational motion of the upper mantle, the asthenosphere. However, as stated earlier, there has been evidence presented for nonsynchronous (decoupled) rotation within Europa. So while their claims are not entirely invalid, there are some broad assumptions made for their model to accurately describe what is seen in the data.

[Kattenhorn & Prockter \(2014\)](#) explain the apparent discrepancy between mountain-building on Earth at convergent plate boundaries and on Europa as a difference between an icy and rocky crust. While the terrestrial rocky lithosphere builds mountains over time, they claim an ice plate can be entirely subducted without creating topographic changes. Again, this relies on the ice being either ductile or brittle. A brittle ice would be incapable of mountain building, as the tensile strength of the ice is not sufficient to support large-scale mountain building. A ductile ice may be capable of storing energy and building upon itself without breaking, but the mountains could not be as tall as those observed on Earth. However, if the plates are thin and therefore the subduction rate is faster, the speed itself may be enough to inhibit mountain building. In a thicker plate/slower subduction rate scenario, there may be a surface downwelling near the subduction zone, which may have formed various chaos terrain features across Europa ([Schmidt et al. \(2011\)](#)).

The evidence presented by [Kattenhorn & Prockter \(2014\)](#) seems to oppose our initial hypothesis that ridges could be positive topography caused at convergent plate boundaries; however, this isolated study does not entirely rule out the possibility of ridges acting as compressional features elsewhere on Europa. In fact, it is possible that there are many different active formation mechanisms at play to create the wide variety of ridges we see in Galileo images. The future of modelling tectonic processes and the interior of Europa will follow from these types of studies, especially in the field of finding relationships between different feature types.

## 2.5 Surface Geology

### Band Formation

Bands are thought to form through episodic tectonic plate separation, and begin as a single crack in the ice which acts as a central trough (Gaidos & Nimmo (2000)). Each plate separation event results in the formation of a pair of symmetrical ridges (positive topography with high albedo) forming on either side of the central trough. In short, some force drives the plates apart, material is ejected, freezes, and this cycle repeats so long as the plates have sufficient energy to drive the plate motion. The ejected material could be sourced from the liquid water ocean, which be possible if the ice shell was thinner ( $< 5\text{km}$ ) but less likely if there was a thick ice shell ( $> 5\text{km}$ ), as separating a thicker plate would require significantly more energy to drive subduction.

In the case that the ice shell is thick, a liquid source for bands could still be obtained through pockets of water within the ice shell. Isolated regions of liquid water within the icy shell has been predicted through models of chaos terrain formation, where thermal plumes from the interior travelling outward to the surface have sufficient heat to melt the ice. If the plumes runs out of thermal energy before reaching the surface, a pocket of water could form before gradually freezing. This explanation could also explain why bands stop expanding: maybe the water creates an instability in the crust which allows for separation (driven by tidal fluxes, or tectonic activity elsewhere on the surface), but as the water freezes, it becomes more difficult for the plates to separate and eventually their motion ceases.

Pockets of liquid water could also also form in new crust, as when salty water freezes it tries to eject the salt to form mostly pure  $\text{H}_2\text{O}$  (Greeley et al. (1998)). As more water freezes, the remaining volume of water becomes saltier, and may become trapped pockets of brine which have a lower freezing point than pure water. This model would be directly testable if we were able to map the chemical spectrometer data directly onto the surface, but attempts at this have been so far unsuccessful (Geissler et al. (1998)). Also, seeing as we do not know the salt composition of the liquid water ocean, it would be unclear whether detection of

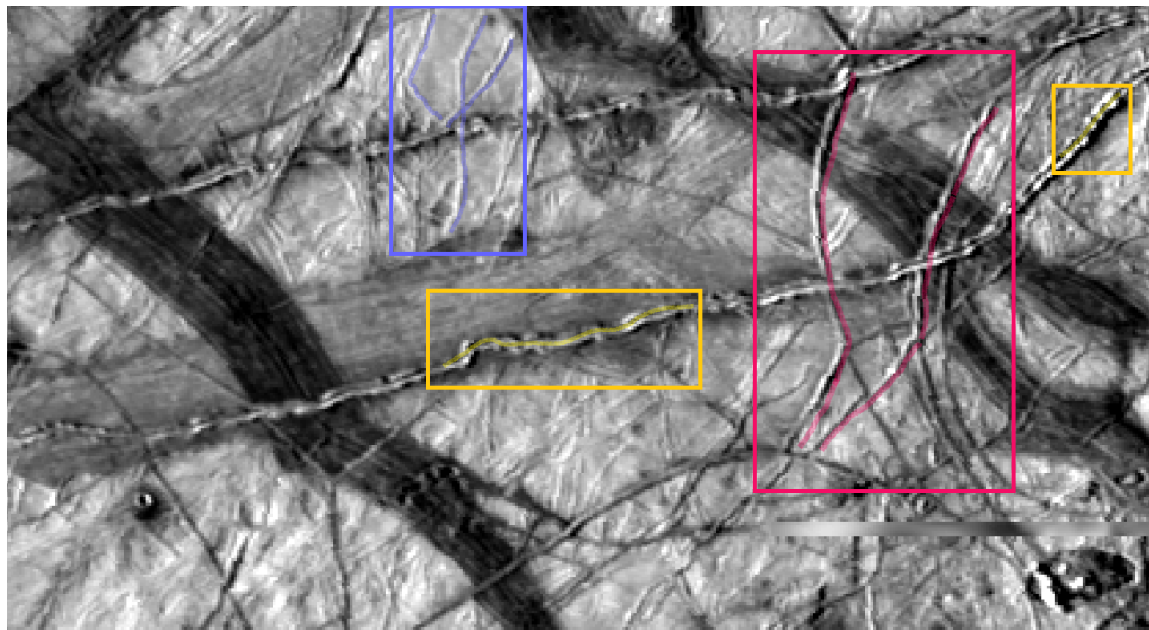


FIGURE 2.8: This image from Site 1 includes single ridges (blue), cycloidal ridges (red) and double ridge (yellow). Double ridges have a measurable depression (shadow) through the center of the feature, while single ridges appear to have a singular peak with accompanying shadow.

salts in bands is indicative of their source being pockets of brine within the shell or a salty ocean.

### Ridge Formation

As previously stated, ridges are high-albedo features with positive topography which we hypothesize may act as complementary compressional features to the extensional bands. Various types of ridges are shown in Figure 2.8 and include single ridges, double ridges, multi-ridge complexes, and cycloidal ridges.

When it comes to theories surrounding the formation of ridges, there are at least twelve key features which must be explained by any proposed model (Head et al. (1999)):

- (1) their linearity
- (2) their great lateral extent and consistency in morphologic form,
- (3) their positive topography
- (4) the upbowing of some background ridged plains features in the formation of their outer ridges

- (5) the formation of marginal troughs
- (6) the formation of washboard texture and margin parallel fractures
- (7) the formation of inner ridges
- (8) the detailed nature of their outer and inner slopes
- (9) their continued formation with multiple, sequential orientations
- (10) their color characteristics
- (11) their relationships to other features
- (12) the potential significance of their arrangement in a classification scheme from simple troughs to complex ridges

Needless to say, the process is likely made up of many component processes over geologic timescales. While there is a fairly straightforward and accepted model of band formation through plate separation, theories which hypothesize on the processes surrounding ridge formation are highly complex and variable. There is no singular model which is able to explain the formation of all observed types of ridges, so it is possible that each ridge type has unique formation mechanisms, which might vary based on geological conditions.

### **Formation Models: Ejecta**

Many of the most detailed models for ridge formation predict ridge formation not through compression as we are exploring, but through the buildup of ejected material. [Geissler et al. \(1998\)](#) propose a life-cycle of ridge formation, and they begin by defining several key features: triple bands are low to moderate albedo features with a bright central stripe, and lineaments are extensional features affected by orbital mechanics (tidal flexing, long-term orbital evolution, and nonsynchronous planetary rotation). The authors propose that triple ridges begin as lineaments, which form as fractures with a slight positive elevation at brittle points in the crust. Ridges on the margins of this initial crack— called marginal ridges — are built as material is ejected over time.

[Geissler et al. \(1998\)](#) explain the likelihood of a crack transforming into a double ridge is related to the speed of the ridge-building process, which is likely dependent on a number of factors like internal convection rate, locations weakness or instability in the crust, the chemical composition of surface ice, and tidal flexing via orbital configuration. It is possible that a combination of these factors could be

at work in the formation of large ridges or ridge complexes. Ridges will continue to build until their weight exceeds the limit that can be supported by the crust, which bends and buckles in compensation. In some cases, these weaknesses may propagate to create parallel fractures and form multi-ridge complexes. In short, this theory of ridge formation relies on an active crack in the crust ejecting material which piles up. In this model, there is no active compression at work, aside from the tidal flexure the crack may experience to drive material to be ejected. The type of ice in this ridge may be more porous and less dense than the surrounding ice, and this porosity may be evidenced by reddish-brown colored contaminants leaking from the ridges into the surrounding ice (see Figure 2.10).

A simple explanation for ridges comes from [Head et al. \(1999\)](#), who propose a model of Europa with a dual-layered icy shell. There is a brittle top layer of ice, and ductile, warmer bottom layer of ice. A preexisting fracture caused by tidal stresses becomes a ridge when a plume of heat called a diapir causes the ice to melt, bend and fault at the surface. This process of ridge formation where the initial fracture is caused by tidal stresses, and the ice shell is segmented into a brittle top layer and a ductile, warmer bottom layer. A linear diapir upwelling causes the ice to melt, bend and fault at the surface, which accounts for many of our current observations.

Examining the highest resolution (20-30 m/pixel) images of ridges reveals some important details. Ridges have an inner, shorter slope and an outer, longer slope. They can also be accompanied by low albedo troughs, which appear to have consistent width at low resolutions, but their varying depth and widths can be observed at higher resolutions.

[Head et al. \(1999\)](#) categorize the outer ridges into four components (see Figure 2.9). The first, uppermost feature makes up half to two-thirds of the outer wall width, and has a rough texture. The second is the low-albedo terraces flanked by higher-albedo scarps (very steep slopes). The close proximity of scarps and terraces could be used to interpret them as slump terraces and faults, where material falls off steeper slopes and will expose younger, brighter material on the slopes. As the scarps appear in steeper regions, their brightness may be caused by the exposure of fresh material. The third unit is uniformly smooth with relatively intermediate

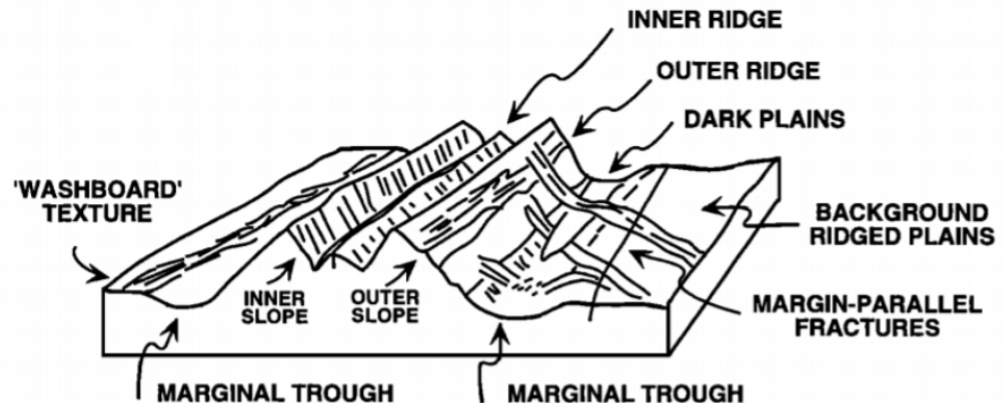


FIGURE 2.9: (Figure from [Head et al. \(1999\)](#)). A block diagram showing a triple-ridge system and the four components of the outer ridge: the rough-textured top, the low-albedo terraces and higher albedo scarps, the smooth intermediate albedo component near the base, and the hummocky "washboard texture" at the base of the slope.

to low albedo. The material shed from the previous region could accumulate in this third region, which would explain the difference in albedo. Finally, the fourth section is a hummocky (extremely uneven) low-albedo deposit at the base of the slope, which could be interpreted as local accumulation of the larger blocks of debris at the bottom of the slope.

Based on these observations, the outer slopes of the outermost ridges were once a part of the background plains, but have been tilted upwards and modified by several processes including faulting, terrace and scarp formation (with the possibility of mass-wasting events), and debris modification and burial towards the base of the ridge. There are also likely processes involving brightness and color modification to match the observations, although there is not yet a specific mechanism proposed, a possible modification to change the color would be changes in grain size of the ice, or the removal of volatile materials.

[Greenberg et al. \(1998\)](#) propose a mechanism for double-ridge formation involving the orbital mechanics, where these features form from existing cracks in the surface which may propagate and form positive topography from the frequent diurnal tides. Due to the high-frequency of these tides, double-ridges could be built on a relatively short timescale.

Color observations from Galileo suggest that ridges are extruded as relatively clean, uncontaminated water ice, while the darkness of bands indicate some sort of contamination, likely a salt or other pollutant from nearby volcanic moon Io (Geissler et al. (1998)). Additionally, some ridge complexes darken and redden the adjacent surface, while the ridges remain at a high albedo. Several theories for their formation have been proposed. The material could be crystallized briny water (with Mg- and Na-sulphates) erupted from the subsurface (Grasset et al. (2013)). These features could be explained by hydrated sulphuric acid formed by radiolysis, a process where a molecule (in this case, water and a sulphur compound) is dissociated by high-energy radiation, often in the form of alpha particles. They could also be explained by hydrated salts, and in the case that contamination of the surface near ridges formed as a combination of sulphuric acid and salt hydrates, the mechanism could be that the sodium associated with some salts could undergo radiolysis, where abundant  $H^+$  ions could replace them to form sulphuric acid. The abundance of hydrogen ions is attributed to the pollution originally ejected from Io (Geissler et al. (1998)).

### Craters

Europa's tectonically active surface presents a problem, as one of the simplest methods of determining the age of solar system bodies involves analysis of the cratered surface (Bierhaus et al. (2005)). The general lack of impact craters was the first indication of the young surface age, which was one of the first properties that made planetary scientists interested in Europa, as there had to be some active mechanism at play to recycle the surface content. This means that if the surface is constantly being broken and reformed through tectonic processes, craters dating back to the initial formation of the moon may have already been destroyed. While there are many constraints to this method of dating (erosion rates, crater saturation, atmospheric conditions, variable crater formation events), it may be used as a simple and qualitative preliminary age measurement. Based on the low spatial density of craters on Europa, it is estimated that the surface is about 60-90 million years old Leonard et al. (2018).

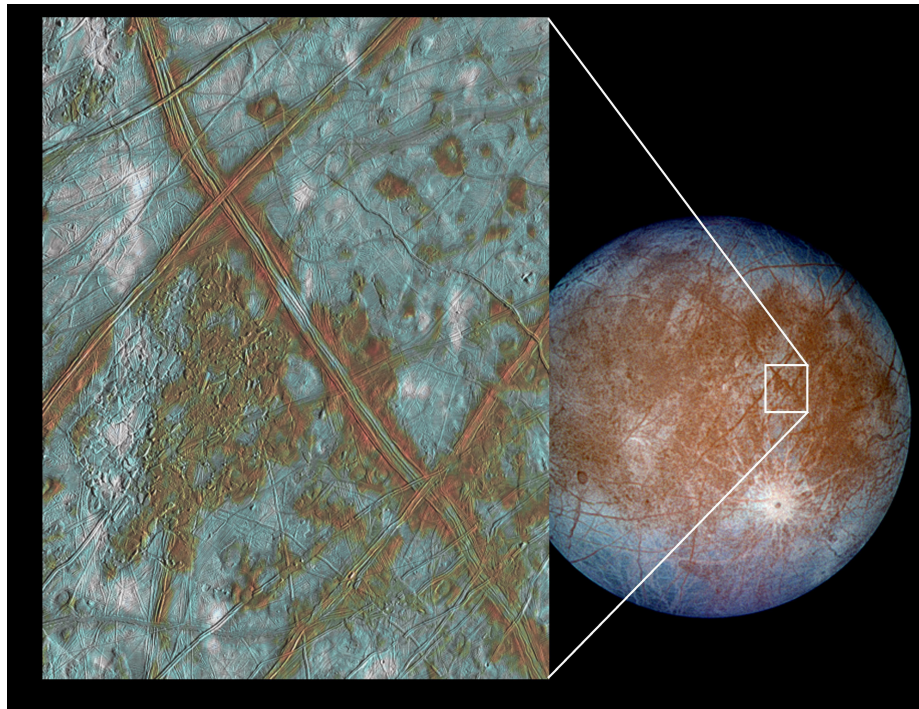


FIGURE 2.10: The image on the left shows Conamara Chaos, a region of Europa's surface where some process has disrupted the preexisting terrain of cross-cutting ridges. In this false-color image, reddish-brown areas represent impure ice. White areas are rays of material ejected during the formation of the 25-km diameter impact crater Pwyll (see global view). Ice is blue, and coarser-grained ice is darker blue while finer-grained ice is light blue. Image credit: NASA/JPL

### Chaos Terrain

Another surface feature that troubled astronomers were chaos terrains like Conamara Chaos and Thera Macula, which became famous after the Galileo spacecraft close-approach flyby in 1997 (see Figure 2.10 and 2.11). Chaos terrain is a term used in astrogeology to define a region where surface features are mixed and dispersed across other regions of independently forming features (Schmidt et al. (2011)).

While Conamara Chaos and Thera Macula are both classified as chaos terrain, they have very different topographies. Conamara Chaos is raised into rounded domes while Thera Macula is a depression in a mostly level surface. Based on similar Earth analogues, the authors suggest a four-phase lens-collapse model shown in Figure 2.12, where both features can be formed via the same process and are examples of stages (c) and (d).



FIGURE 2.11: The image taken by Galileo at 220 m/pixel resolution shows Thera Macula, a depressional feature which suggests there could be liquid water below its surface. Image credit: [Pappalardo et al. \(2013\)](#)

Warm, buoyant plumes of heat from Europa's interior move outwards from the surface through the process of convection, which is presumed to function similarly to convection processes in Earth's mantle. Convection is a cyclical process where material near the core is heated by the residual heat of formation and energy generated through radioactive decay of elements- in short, the core is warmer than the outer layers. Cooler, denser material from above falls down towards the core, heats up, becomes less dense and more buoyant and rises away from the mantle, then the material gradually cools and the process repeats.

Plumes of heat generated via convection could create volumes of partially melted ice (called lenses) within the ice crust. The round shape of the plume produces a round lens of ice, which refreezes from the bottom up as the energy from the plume dissipates. This process could be thought of in the same way as blowing a

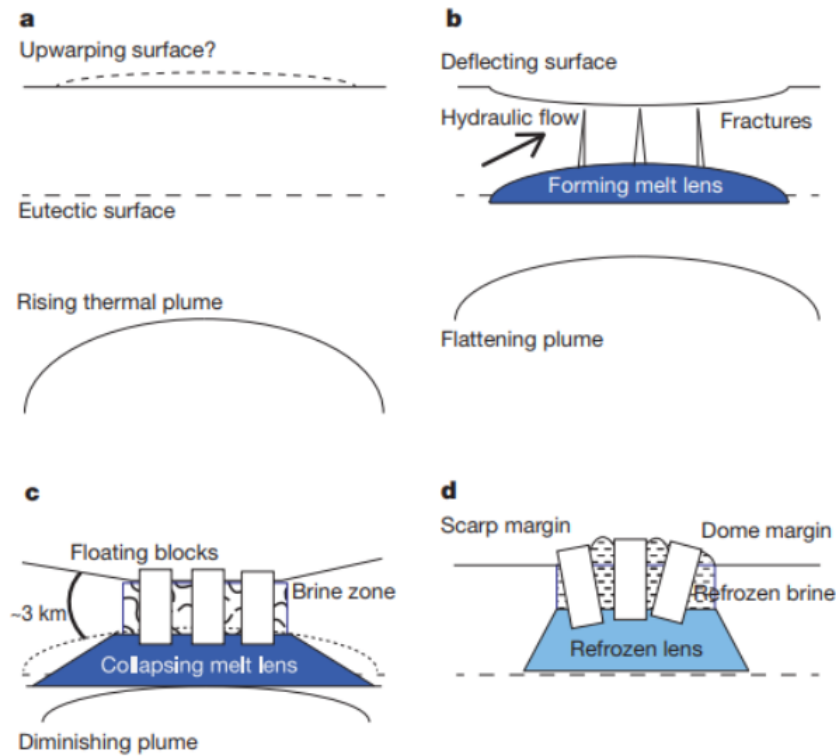


FIGURE 2.12: (Figure and caption (modified) from Schmidt et al. (2011)): (a) An ascending subsurface thermal plume approaches the pressure-melt point of the overlying impure brittle ice. (b), Melting causes subsurface subsidence that hydraulically confines the water and produces tensile cracks. (c), Hydrofracture from the melt lens causes ice blocks to break off the edges while fracture and brine infiltration form a granular matrix. (d), Refreezing of the melt lens and freezing of now brine-rich matrix raises the chaos feature above surrounding terrain, and can cause domes to form between blocks and at margins.

soap bubble: the bubble will continue to grow until you stop blowing, just as the meltwater lens will continue to grow until the thermal plume diminishes, and the lens will re-freeze at the bottom without the plume's source of heat. Ultimately, the volume of meltwater and depth of hydrostatic equilibrium (the point below the surface where forces of gravity and pressure balance each other) will determine how much the overlying surface depresses. The composition and thickness of the ice above the lens will determine how the crust will fracture and fault in response to this depression. Cracks propagate upwards from the lens to the surface, and will break off in steep blocks, allowing water from the lens to enter the now brittle overlying ice. This outlines the process which forms surface depression features such as Thera Macula.

In Summary, Chapter 2 has discussed past missions to Europa which have allowed us to better understand orbital mechanics, the existence of a subsurface ocean and the resulting surface features, many of are hypothesized to form through tectonic processes. Of the five types of surface features (bands, ridges, chaos terrain, background matrix and craters), bands are well-documented features with a generally accepted mechanism of formation. Bands form through individual spreading events, where material from the interior leaks out above the surface and solidifies [Gaidos & Nimmo \(2000\)](#). Ridges are less understood, and most proposed mechanisms of formation involve a combination of ejecta through cryovolcanism and tidal interactions between Europa, Jupiter, Io and Ganymede (e.g. [Head et al. \(1999\)](#), [Geissler et al. \(1998\)](#), [Greenberg et al. \(1998\)](#)). There has also been a publication by [Kattenhorn & Prockter \(2014\)](#) which computes the percent surface area (10-40%) in which subduction (compression) can accommodate for new ice created at band spreading. With all of this information, we are ready to move onto discussing the mapping techniques used in this thesis

## CHAPTER 3: Mapping Techniques and Calculations

### 3.1 Mapping Overview

#### Region Selection

There was significant care and planning for the selection of which regions to use on Europa, which are shown in Figure 3.1. A non-random selection process would introduce an element of bias which must be addressed into our analysis. For example, if I selected only regions in the northern hemisphere near the pole, it would be difficult to interpret our data on a global scale. Therefore, I tried pick sites across various longitudes and latitudes in order to obtain a more global representation. Unfortunately, the majority of surface coverage of the global mosaic relies on the lower-resolution Voyager data. As many ridges were undetectable at this resolution, I was limited to using regions with Galileo's moderate-resolution data, which

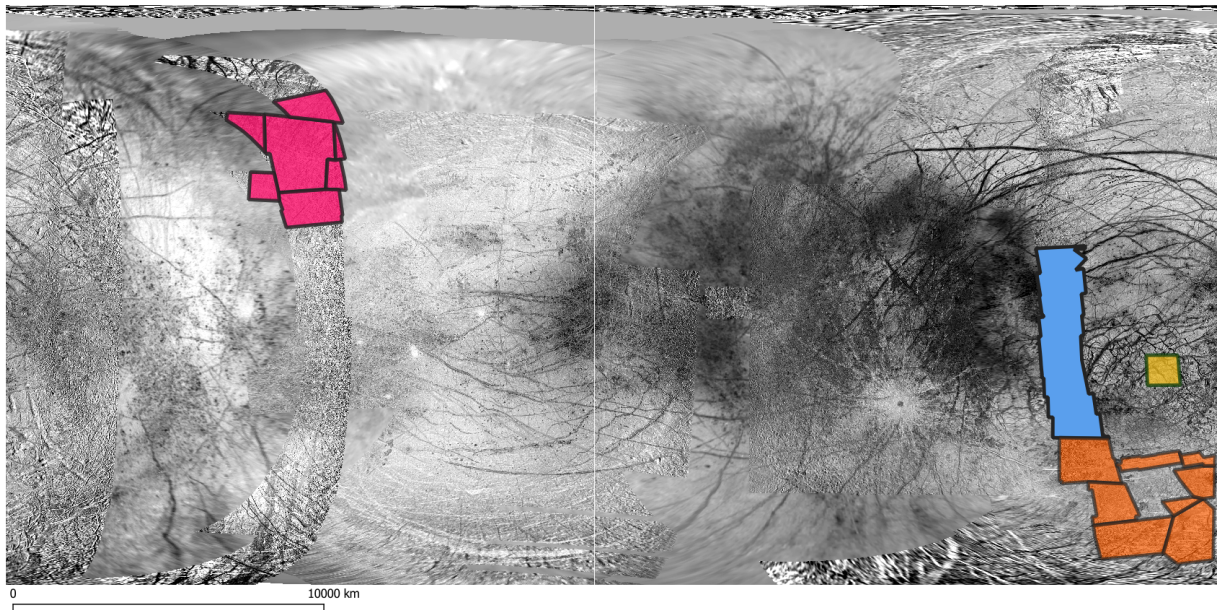


FIGURE 3.1: Global mosaic of Europa Sites 1 (yellow), Site 2 (orange), Site 3 (pink), and Site 4 (blue). These sites account for 4.62% of Europa's total surface area.

comprise less than 25% of the total surface coverage. Of this smaller subsection of the surface, I was also limited to using the highest resolution available on the global mosaic, which at best was around 200 m/pixel.

Even if a region had the higher resolution I was looking for, the solar incidence angle of the region was another factor I had to consider. Shown in Figure 3.2, the solar incidence angle of the left image is nearly  $0^\circ$ , meaning the Sun is almost directly overhead at the time the image was taken. Ideally, to minimize error I would choose regions with the highest solar incidence and therefore longest shadows, as the fractional uncertainty would be smaller in longer shadows compared to shorter shadows. However, at the resolutions given, with most ridges having heights of 1 km or less, it is unlikely that a  $30^\circ$  change in incidence angle could create an observable change in the shadow ( $>200\text{m}$  difference with resolutions at 200 m/pixel). The high solar incidence also makes the surface appear to reflect more light, making it difficult to distinguish the positive topography of ridges or high albedo (older) bands from the surrounding terrain. Additionally, some major features become undetectable at high incidence angles (where viewed from on the surface, the sun is near the horizon), such as the ancient band Agenor that runs through Site 2 (Geissler et al. (1998)). Each of these factors limit our ability to accurately measure ridges, so I found solar incidence angles between  $20\text{-}70^\circ$  generally provide acceptable viewing conditions.

Site 1 was selected first as there have been several publications on this region in the past (Stempel et al. (2005), Leonard et al. (2018), Sullivan et al. (1998)), including a tectonic reconstruction which will provide useful values to compare to my surface area calculations. Sites 2, 3, and 4 were selected somewhat arbitrarily using the described criteria, and were intended to be approximately equal in surface area (around 400,00 square kilometers) to see how ridge-band ratios compare in regions of similar sizes that are geographically separated. However, sites 1, 2 and 4 are in relative local proximity, which is not ideal global interpretations of this data, but this area contained moderate-resolution Galileo images at ideal solar incidence angles, and so were selected in favor of regions which were spaced further apart but offered poor contrast at low solar incidence angles.

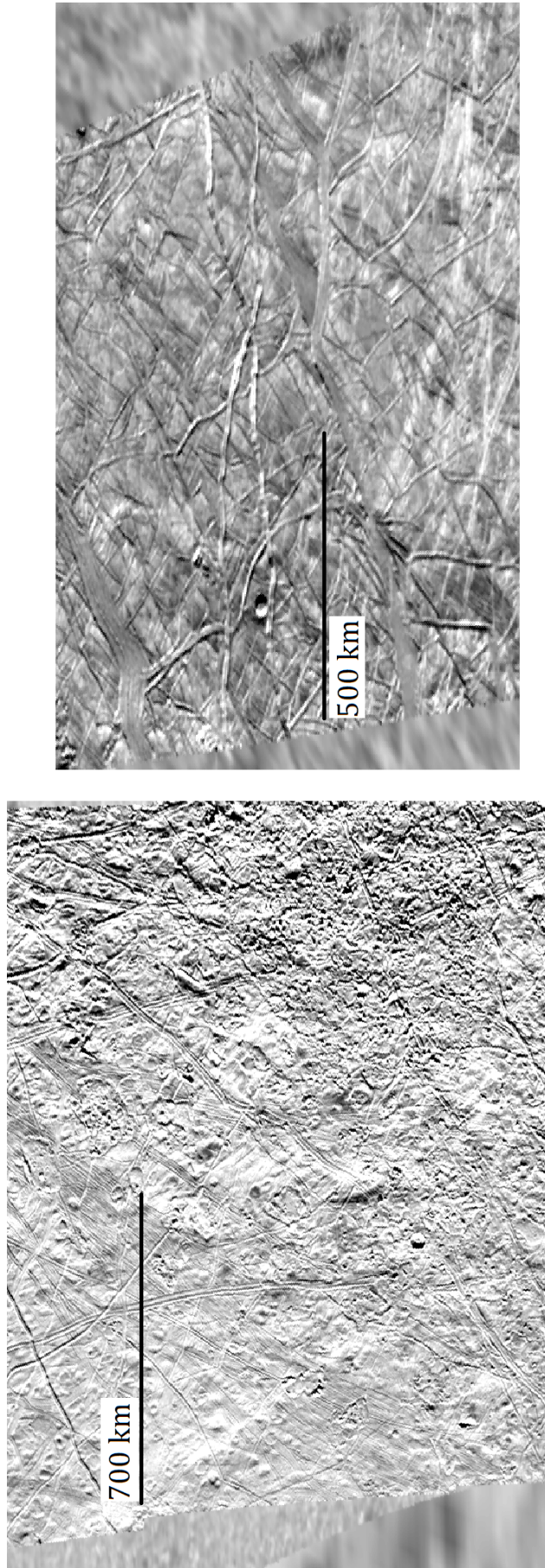


FIGURE 3.2: Comparison of two regions of Europa, where solar incidence angle of the left image is nearly  $90^\circ$ , meaning the Sun is almost directly overhead at the time the image was taken. In the image on the right, the solar incidence angle is  $\approx 25^\circ$ . While I could adjust the contrast of the brighter image, this mosaic was processed in a way that conserved the original contrast, so altering the it could produce changes that I have no way to factor into our results. For example, the inconsistency may mean I could identify and measure shadows differently in these washed-out regions. The major focus with mapping was to keep the process consistent in order to minimize bias and make our results reproducible. Therefore, I viewed and mapped all sites at the default contrast levels.

## 3.2 Classification of Surface Features

### 3.2.1 Ridge Classification

While there are numerous identifying characteristics for ridges (see Section 2), few of them are visible at even the moderate-resolution regions of the global mosaic. Therefore, I am able to define ridges quite simply as high albedo, semi-linear features with an accompanying, measurable shadow shadow (at least 1 pixel long). While our criteria is straightforward, there were various elements which complicated the mapping process.

First, the orientation of the ridge determines the direction of the shadow. Maximum shadow length will be achieved when the ridge is oriented perpendicular to the sun. Figure 3.3 shows Site 1 with location of the Sun obtained from the regions label file, provided from the US Geological Survey (USGS). These label files provide useful information about the solar incidence angle and spacecraft position, which I used to determine the location of the Sun relative to the surface when the image was taken.

There were only three necessary measurements for calculating ridge volume and surface area: the total ridge length, average width, and height. Ridge length was measured directly through the center of the feature. Ridge widths were measured along evenly spaced increments, and a median width was determined for each ridge, this value used for volume and surface area calculations. Heights were derived using the shadows cast from ridges. For consistency, shadows were measured from the center of the ridge to the edge of the shadow, and all shadow measurements were made perpendicular to the parallel lines indicating solar position. I later subtract half the ridge width from this shadow to find the true shadow length. This method of measuring shadows is more precise than measuring shadows from where they begin adjacent to the ridge to their end, and allows for greater consistency in measurements that are independent of a ridge's slope angle. An example of view of shadow measurements is provided in Figure 3.4.

Even with the highest resolution images on Europa, it has not yet been possible to determine exact topographic shape or slope of the ridges. There is also

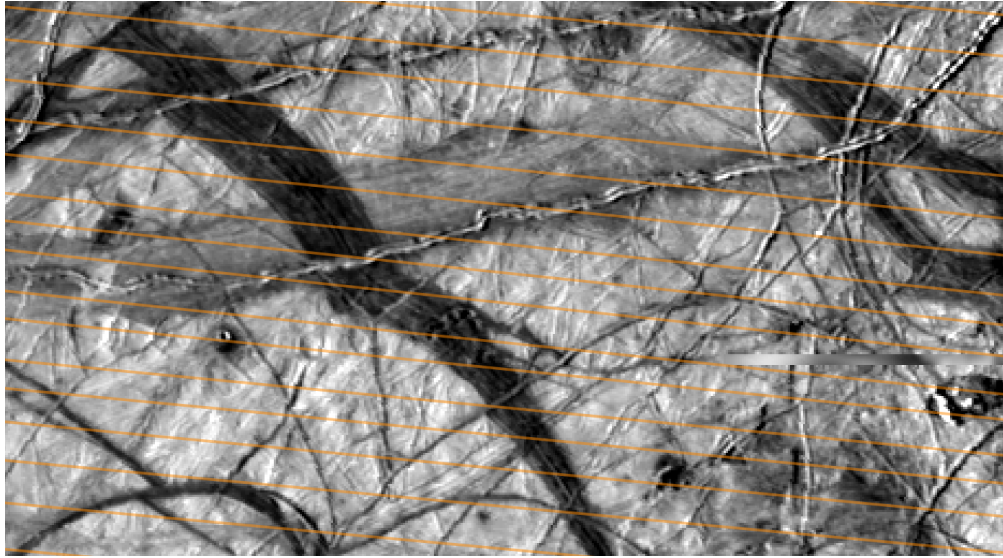


FIGURE 3.3: Site 1 with the sun oriented almost directly west (left) in the image. Parallel lines indicate the relative direction of the Sun, referenced from the center of the site. Notice that the most prominent shadows come from ridges that are oriented perpendicularly (north/south) to the direction of the sun, and smallest for ridges oriented parallel (east-west).

uncertainty in their formation, as ridges within a given region may have entirely different formation mechanisms (Johnston & Montesi (2014)). In this work I considered three plausible geometric models of ridges: triangular, rectangular, and ellipsoidal ridges. Triangular ridges can be thought of as similar to the mountains we see on Earth, which can be roughly approximated as triangular prisms. This model appears to favor observations of multi-ridge systems at high resolution. The rectangular model shows ridges as steep-sided and flat-topped plateau features, which is thought to be the most realistic representation based on current observation (Greeley et al. (2000)). Finally, an intermediate model between triangular and rectangular is the rounded hill-like morphology of the ellipsoidal model (Johnston & Montesi (2014)). While these models only create small variations in volume and surface area for individual ridges, when examining an entire region these variations become significant.

Finally, I include examples of surface features which appear ridge-like but could not be mapped in this study. Troughs, which are dark, skinny linear features which often accompany ridges, can be easily mistaken as a shadow. Figure 3.5 shows an example of a ridge with an accompanying trough that is longer than the

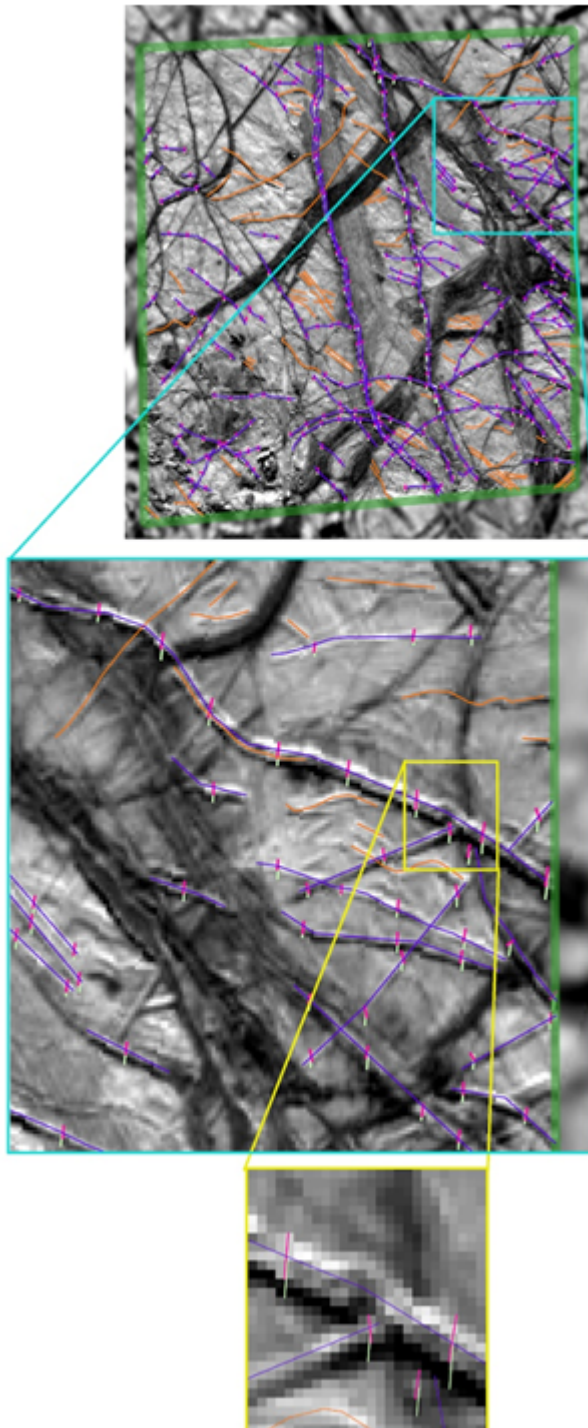


FIGURE 3.4: Site 1 with overlaid shadow and width measurements made in even 10km increments. If a shadow could not be found between two width increments, a value was not recorded for the average. At this site alone, 181 ridges were mapped with 1058 individual shadow length and width measurements.

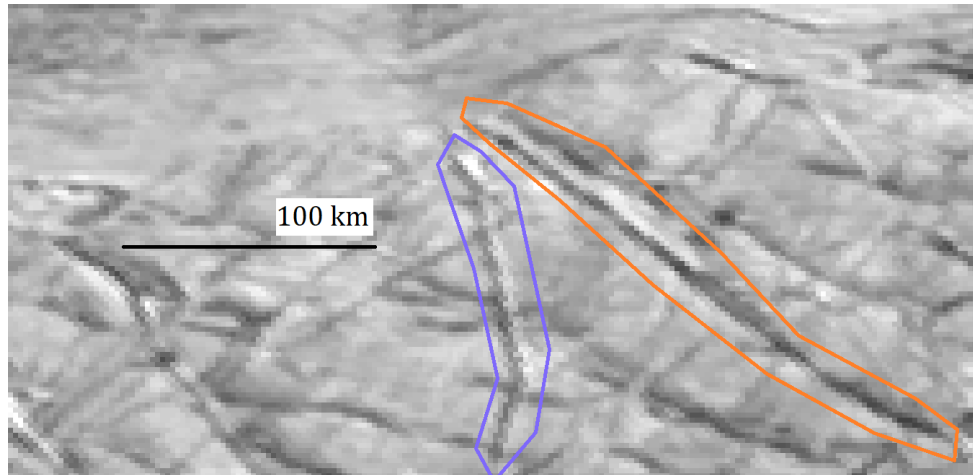


FIGURE 3.5: This region of Site 2 shows a proper ridge feature outlined in blue, as well as a ridge-like feature outlined in orange with an accompanying trough. Given the orientation of other shadows in this image, the trough could be easily mistaken for a shadow, but ridges are only mapped so long as they have a paired positive topography with a measurable shadow.

body of the ridge itself. In these cases, the ridge was only measure as long as there was measurable positive topography and an accompanying shadow. Additionally, some positive albedo features have no accompanying shadow. In this case, there may be differences in the material which allow it to have higher albedo but not necessary positive topography, and thus cannot be classified as a ridge. In cases where the orientation of the ridge with reference to the position of the sun caused a shadow to be blocked, like with an east-west oriented ridge and the sun directly west in the image. there are be fewer opportunities to accurately map shadow lengths. Therefore, I rely on the small deviations north or south which create a measurable shadow.

### 3.2.2 Band Classification

The main challenge of band identification is their variation in color and size. Bands can exist across a wide range of albedo, which is a measure of brightness and reflectivity of a material. Bands can be white, light-gray, charcoal, and nearly black, and their appearance has been linked to their age (Pappalardo et al. (1999)). The geological law of superposition provides a method of relative age-dating, as it predicts that if material is deposited at the surface in layers, then the youngest

material is in the top layer and the oldest are on the bottom. Therefore in a stack of 3 overlaying bands, the youngest band would be on top, while the oldest band would be at the bottom (see Figure 3.6). Based on this principle, geologists have been able to infer that younger bands are darker when they are first ejected, appear to gradually lighten over time, perhaps by the bombardment of particles from nearby volcanically active moon Io (Geissler et al. (1998)). In general, I define bands as extension features which differ in color from the surrounding terrain, and are thick enough to have evidence of symmetric positive topography indicative of individual spreading events.

### 3.3 Models for Calculation

#### 3.3.1 Bands

There are two models of band spreading which can lead to significantly different volume calculations: triangular and rectangular wedge geometries (Prockter et al. (2002) and Stempel et al. (2005)). In the triangular model, the plates are pushed apart from a central point into a shape that creates a triangular prism of new crust (see Figure 3.7). The rectangular model predicts the plates pull apart entirely to create a rectangular prism a consistent width at any given depth. Both models require a known depth where the spreading originates for calculations, but the thickness of the ice shell is still debated. Therefore, I searched the literature for proposed values of shell thickness, and found values between 100 m to 50 km have been used (Billings & Kattenhorn (2005)). Obviously, this provides a wide range of possible values, and demonstrates the innate challenge of trying to find an estimate for ice thickness.

In Section 5 I list several ice depths from 100 m to 50 km and calculate volumes at various depths. As all of these models for both bands and ridges are plausible, calculations were performed using each of the three models for ridges and two for bands.

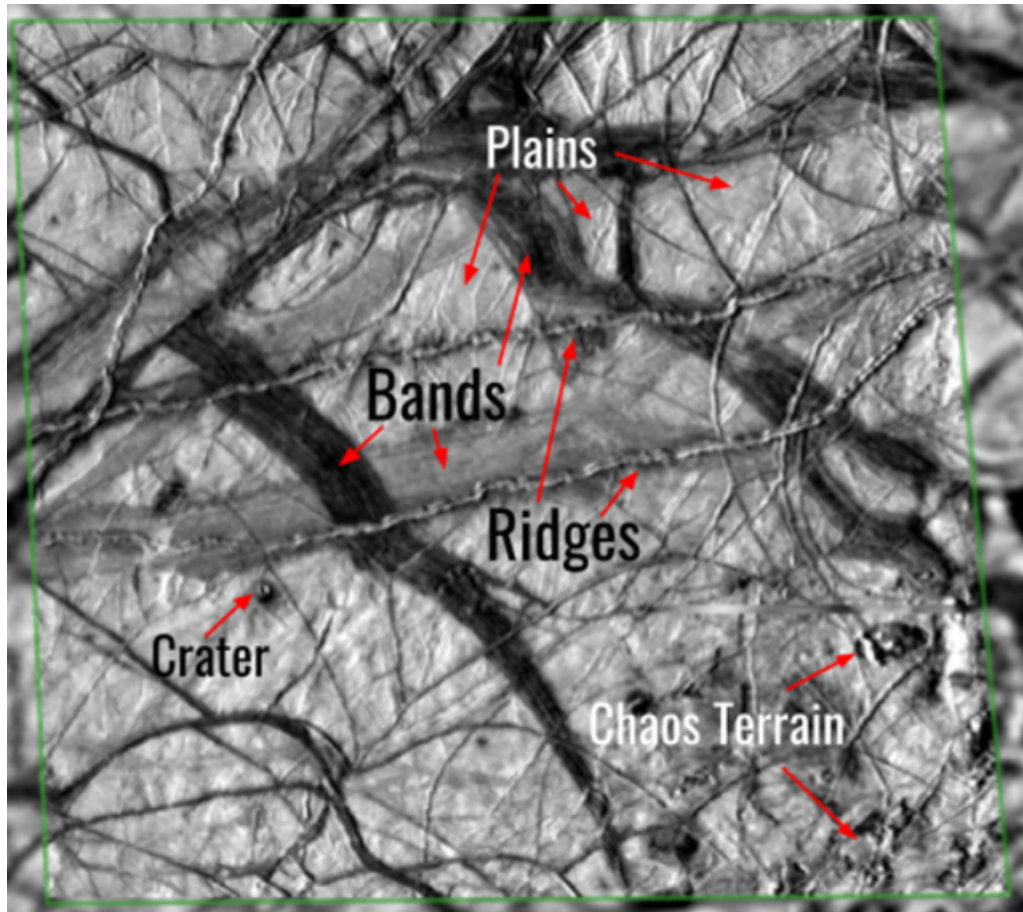


FIGURE 3.6: Site 1 before mapping. All 5 types of surface terrain can be seen here: bands, ridges (including double ridges), craters, chaos terrain, and plains. Note that the bands have a wide range of albedos, with the darkest in the middle overtop an older, faded band. There are several distinct double ridge systems in this image, with two running nearly horizontal and parallel through the center. The chaos terrain was not mapped for the purposes of this study, although some propose that the chaos formation mechanism may be linked to certain ridge formation processes (Schmidt et al. (2011)).

### 3.3.2 Height from Shadow Length

Shadow lengths were measured from the center of the ridge to the end of the shadow, shown in Figure 3.4. Each site consists of one or multiple images mosaicked together from multiple flybys. The label files of these images are publicly available via the USGS, and contain information about the solar incidence angle ( $i$ ) during the time of the image. With this angle, we are able to use trigonometry to calculate the height of a ridge given its known shadow length ( $s$ ) using the

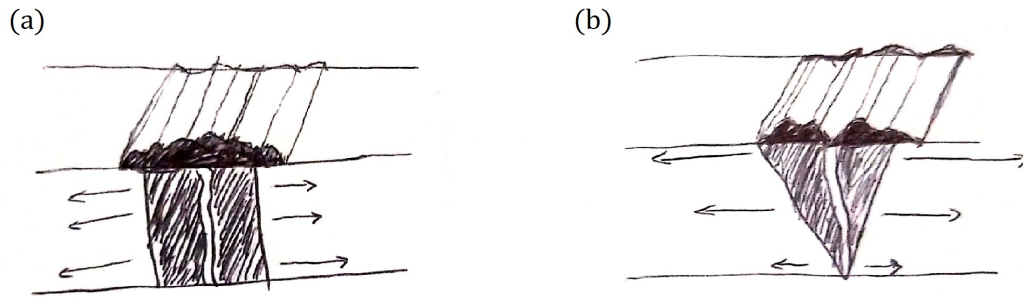


FIGURE 3.7: Shows the rectangular model (a) versus the triangular model (b) for band extension. Arrows indicate how a variable stress field could cause a triangular band to form, where the force is greatest at the surface and decreases with depth. For the rectangular model, these forces would have to be mostly consistent, although likely would need to increase slightly with depth for the force to accommodate the greater weight of overlying ice at greater depths.

following equation:

$$h = \tan(i)(s) \quad (3.1)$$

### 3.3.3 Triangular Ridges

In order to calculate the surface area of the triangular geometry, I approximated the ridge as a triangular prism and calculated the area of the two exposed sides.

$$SA = 2l\alpha \quad (3.2)$$

where  $\alpha$  is the length of one side of the isosceles triangle and can be calculated using simple trigonometry. Splitting the isosceles triangle in half to create two right triangles allowed us to solve for the bottom non-right angles ( $\theta$ ) with the known height ( $h$ ) and base ( $0.5w$ ) of the triangle.

$$\theta = \arctan\left(\frac{h}{0.5w}\right) \quad (3.3)$$

With this solved angle,  $\alpha$  can be found using  $h$  and  $\sin \theta$

$$\alpha = \frac{h}{\sin \theta} \quad (3.4)$$

The volume in this triangular ridge model is approximated by the volume of a triangular prism:

$$V = (0.5wh)l \quad (3.5)$$

### 3.3.4 Rectangular Ridges

The surface area of a rectangular ridge includes the top and two sides of the ridge:

$$SA = (lw) + (2lh) \quad (3.6)$$

The volume is simply the volume of a rectangular prism:

$$V = lwh \quad (3.7)$$

### 3.3.5 Elliptical Ridges

In the rounded ridge morphology, the ridge was approximated as half an ellipse, the surface area calculated using the Ramanujan approximation for the perimeter of an ellipse (Almkvist and Berndt, 1988):

$$SA = 0.5\pi l \left[ 3(0.5w + h) - \sqrt{(3(0.5w) + h(w + 3h))} \right] \quad (3.8)$$

The volume is given by half the volume of an ellipsoidal cylinder:

$$V = 0.25\pi = whl \quad (3.9)$$

### 3.3.6 Rectangular wedge

The rectangular wedge is a simple calculation, as the surface area of the bands are automatically calculated in our mapping program (QGIS):

$$V = (SA)(d) \quad (3.10)$$

### 3.3.7 Triangular wedge

In this model, the area of the triangular shaped wedge can be calculated using the average width ( $w$ ) and given depth ( $d$ ), and multiplied by the band length ( $l$ ) to obtain a volume:

$$V = 0.5wdl \quad (3.11)$$

## CHAPTER 4: Data Analysis

---

### An Imperfect Model

We started this project with the understanding that there would be many limitations to our analysis: after all, with this data being nearly 2 decades old, if it was easy someone would have already attempted it. Based on the resolution of available images, the uncertainty of our measurements would be significant. Additionally, the surface area and volume models used for calculations are based on generalized, perfect geometries. In reality, Europa's surface is chaotic, hummocky, and complicated. In this section, I will discuss some large and small scale details, and the effect they may have on our results presented in the previous section.

A detail which deviates from this “perfect” model is the large-scale tidal warping. [Greeley et al. \(1998\)](#) incorporate the concept of a downwarping crust during ridge formation, as the increased density of compacted ice can cause a local depression (see [Figure 4.1](#)). Their model explains the appearance of parallel cracks alongside ridges, as a result of the stress of this crustal warping. Interestingly, their model relies on both cryovolcanic and tectonic processes. Few published papers discuss the possibility of ridges forming solely through compression, though there are many which model ridge formation through cryovolcanism ([Geissler et al. \(1998\)](#), [Head et al. \(1999\)](#), [Greenberg et al. \(1998\)](#)).

For the volume calculations presented in [Chapter 5](#), we assumed the ridges acted as perfect rectangular, triangular, or ellipsoidal prisms. The shape of ridges on Europa is highly dependant on the formation mechanisms and the ice composition. Unfortunately, exact chemical composition of the various surface features is one of the greatest gaps in our knowledge of Europa. If Europa's ridges do not differ in composition from surrounding background matrix, it would support our hypothesis of ridges forming via compressional forces. If the ridges had high salinity in comparison to its surroundings, it is perhaps more likely they formed via cryovolcanism processes (discussed in [Ch 2](#)). However, chemical composition alone is not enough evidence to confirm a theory of ridge formation, as chemical contaminants from the Io could create the hydrated salts we observe ([Geissler et al. \(1998\)](#)).

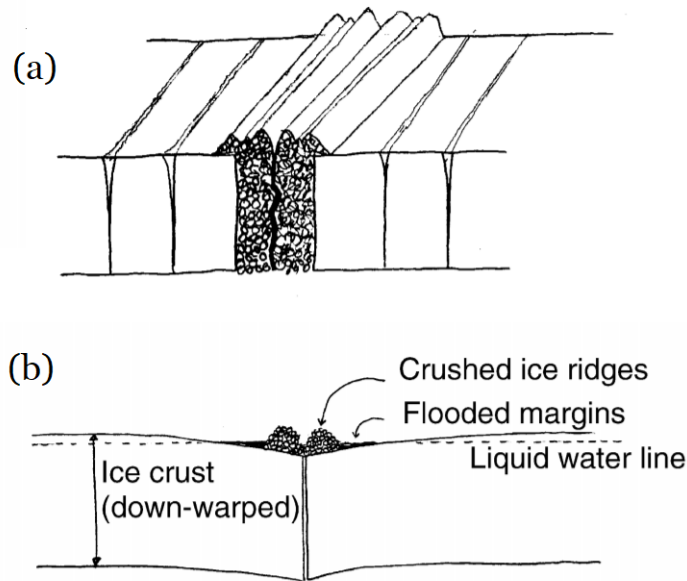


FIGURE 4.1: Image modified from Greeley et al. 1998. (a) shows lateral parallel cracks which form as a result of the downwarping stress. (b) shows how if the weight of the ridge warped the crust to the point where part of the surface lies below the liquid water line, water may stream through the porous ridge ice and create the reddish-brown coloration near global ridge systems seen in Voyager images.

In Chapter 2, I mentioned that the exact composition and behavior of ice across the global surface is still debated. Some studies have cited evidence for a cold, brittle layer overlaying a warmer ductile ice layer which may undergo convection (Kattenhorn & Prockter (2014)). This ambiguity hinders our ability to fully interpret our volume calculations, as we do not account for different densities of ice in this model. A commonly proposed mechanism for double ridge formation is through a cryovolcanic process discussed in Chapter 2, where ejected material form symmetrical hills alongside a central crack. In this case, a porous mountain feature might form, which explains some of the observed discoloration around some of these features (see Figure 2.10, where some ridge complexes exhibit this discoloration).

We also note that this study did not map different types of bands or ridges separately. That is to say, a single ridge was mapped the same as a double ridge, triple ridge, and cycloidal ridge. We did not distinguish between these types during

mapping, we were intentional in creating our hypothesis so that all ridges would be measured as compressional features. Attempting to distinguish between different types of ridges at the moderate to low-resolution images of the global mosaic would introduce significant bias, as introducing more categories of classification creates more space for the mapper's interpretation.

Therefore, in order to first explore the most simplistic case where all ridges are compressional and all bands are extensional, we are looking to see if our hypothesis is even feasible. For example, if the surface area calculations for bands and ridges across each site showed that total band surface area was several orders of magnitude greater than the total ridge surface area, our hypothesis would be mostly disproven, and then we would need to take another approach with a more complex model which may account for differences in density or different ridge formation mechanisms. However, this would likely mean involving multiple scientists to map the same locations given the same mapping criteria, which adds great complexity to interpreting our results. If, however, the total band surface area matched the total ridge surface area within 1-2 orders of magnitude, then we could say our hypothesis is plausible, but we would need more evidence (more of the surface mapped) before we could extend our results to a global context.

I mapped each ridge of a multi-ridge system individually if there is a measurable ( $\geq 1$  pixel) distance between the ridges. However, after viewing some of the higher resolution Galileo images that are not included on the global mosaic, it becomes clear that some ridges that were initially interpreted as single ridges could be double ridges, as the moderate-resolution of 200 m/pixel is too low to capture the central depression. This is another reason we did not want to map the different ridge types: in addition to the mapping bias component, the limiting resolution prevents us from efficiently and correctly identifying single ridges versus double ridges on smaller scales.

Overall, our model does not incorporate intricate factors like ice density and crustal warping, and does not categorize different types of ridges separately, mostly due to the limited resolution of Galileo data used in the global mosaic. Our model was kept simplistic in order to examine a broad hypothesis which can be refined over multiple iterations of the scientific process. Future work will likely include these

factors within calculations and mapping, but we have found our simplified model is sufficient for examining our initial hypothesis.

## CHAPTER 5: Results and Discussion

---

Once I had mapped all ridges and bands across four sites, I used an Excel spreadsheet to compute volume and surface areas of ridges using the three models (triangular, rectangular and ellipsoidal) as well for the two models of bands (triangular and rectangular). Once these calculations were complete, I could determine a ratio of volume or surface area for bands versus ridges within each site, reported here as percentages. Note that I do not list uncertainties for the values in these tables, as sources of error and uncertainty will be discussed in Section 6.

### Surface Area Analysis

Table S1 shows the percent surface area of ridges/bands for Sites 1-4. If the whole European surface were similar in surface composition as Sites 1, 2 and 4, then we could predict that ridges would account for ~35-60% of the total band surface area. Site 3 differs in that ridge area accounts for 70-96% of the band area. These results confirm what we observe from the global images, where instead of having a uniform distribution of bands and ridges, Europa's surface may be broken up into more ridge-dominated components (Site 3) and band-dominated components (Sites 1, 2 and 4).

TABLE S1: Percent surface area calculations for ridges/bands.

Site	Triangular	Rectangular	Ellipse
Site 1	40.15%	49.70%	41.95%
Site 2	35.75%	44.12%	38.81%
Site 3	70.16%	96.22%	74.67%
Site 4	46.41%	57.73%	48.74%

Previous work by [Kattenhorn & Prockter \(2014\)](#) use a model of Europa consisting of a thin (several km) brittle layer of ice overlaying a thicker layer of convecting ice. While the authors do not list the specific values for shell thickness that they used, I can assume they used a value somewhere in the range of 5-50 km. With this model, they created a tectonic reconstruction based on the movement of features across fault lines, which showed that compression could account for just 10-40% of the surface area created through band extension. This fits within our results for Sites 1, 2 and 4, as my calculated values ranged from 35-57%. Our results are more in favor of our initial hypothesis that ridge compression could be counteracting band extension.

The overlap in percent surface area calculations between our results and the results from [Kattenhorn & Prockter \(2014\)](#) gives us more confidence in our mapping methodology and analysis techniques. As I've only mapped one ridge-dominated component, it would be interesting for future analysis to map other regions that appear to have fewer bands and many ridges (i.e. ridge-dominated) to see if these values agree with our results for Site 3. Site 3 is also our only site in the western hemisphere, so I could benefit from choosing a ridge-dominated, equatorial region in the left half of the global mosaic.

### Volume Analysis

Table S2 shows the percent volume for the three models of bands versus the two models of ridges. I am able to calculate the volume above the surface ridges because I can estimate their height from shadows, but because there is no widely accepted value for shell thickness, I do not have a singular depth to reference for band volume. Therefore, I chose five values ranging from 100 m - 50 km, which have all been cited in the literature as plausible shell thicknesses.

[Billings & Kattenhorn \(2005\)](#) present a list of 20+ published estimates of ice-shell thickness and sort their list of published estimates into on four categories based on their methods: modelling flexure in an elastic shell, modelling other mechanical methods such as buoyancy and lithostatic stresses, crater analysis, and thermodynamic analysis. Flexure and other mechanical models favor a thinner (<1km) crust while some thermal and crater models predict a thick (20-40 km) crust. Overall, the results of [Billings & Kattenhorn \(2005\)](#) indicate that an ice sheet thickness

on the order of 200 m -2.2 km has been cited the most frequently among the literature, but they cannot yet rule out the possibility of a much thicker (>50 km) crust. A possible explanation to this discrepancy is that the flexure and other mechanical models may be vast underestimates of the total ice shell thickness, as they model a thin layer of brittle ice, which could in principle overlay a thicker (multiple km), warmer convecting ice shell as predicted by [Kattenhorn & Prockter \(2014\)](#). These mechanical models may be measuring the thickness of this brittle layer, but not accounting for the convecting layer of ice beneath.

As shown in the results from Table S2, it seems that an ice thickness of 100-700 m would allow the volume of ridge ice to compensate for band volume. This depth of ice is relatively thin, but fits within published estimations for the thickness of the ice shell, especially those which model flexure, buoyancy and lithostatic stresses. This makes sense, as ridge and band formation is likely connected to these factors. However, some thermal models predict crust thicknesses on the order of 40 km, and I would expect thermal convection to be connected to band and ridge formation as it is the most commonly hypothesized driving force of plate tectonics. I would expect thermal processes to also be directly linked to ridge and band formation, but our results differ from published values with thermal models by 3 orders of magnitude. It is more common to find a shell thickness listed typically on the order of a few kilometers, although some studies list local shell thickness less than 1 km ([Billings & Kattenhorn \(2005\)](#)). It is possible that the band spreading does not begin where the ice shell meets the ocean, so our volume calculations are likely an underestimate of the actual shell thickness.

As shown in Tables S1 and S2, it seems plausible that compressional ridges account for some of the surface created through band spreading. However, there is a high margin of error in these final surface area and volume results, as the limited resolution introduces significant error. Many of the ridges measured were 2-4 pixels wide, so having just one pixel introduces significant (>20%) uncertainty. If the ridges were steep-sided plateau features as in the rectangular model, the widths I measured would be overestimates. If they had more gradual slopes as in the elliptical model, the measurements would have been underestimates. In general, our strategy was to attempt to maintain the most consistent ridge measurements possible given the resolution restrictions.

TABLE S2: Percent volume calculations for ridges/bands using two band geometries: rectangular (rect) and triangular (tri).

Site 1	100m (rect)	100m (tri)	2km (rect)	2km (tri)	10km (rect)	10km (tri)	50km (rect)	50km (tri)
Vol (tri)	44.21%	91.16%	2.21%	4.56%	0.442%	0.912%	0.088%	0.182%
Vol (rect)	88.42%	182.32%	4.42%	9.12%	0.884%	1.823%	0.177%	0.365%
Vol (ellipse)	69.28%	142.85%	3.46%	7.14%	0.693%	1.429%	0.139%	0.286%
Site 2								
Vol (tri)	42.15%	84.75%	2.11%	4.24%	0.442%	0.848%	0.084%	0.170%
Vol (rect)	84.31%	169.50%	4.22%	8.48%	0.843%	1.695%	0.169%	0.339%
Vol (ellipse)	66.22%	133.13%	3.31%	6.66%	0.662%	1.331%	0.132%	0.266%
Site 3								
Vol (tri)	284.3%	468.2%	14.21%	23.41%	2.843%	4.682%	0.569%	0.936 %
Vol (rect)	568.5%	936.3%	28.43%	46.82%	5.685%	9.363%	1.137%	1.873%
Vol (ellipse)	446.5%	735.4%	22.33%	36.77%	4.465%	7.354%	0.893%	1.471%
Site 4								
Vol (tri)	52.34%	125.51%	2.62%	6.28%	0.523%	1.255%	0.105%	0.251 %
Vol (rect)	104.68%	251.02%	5.23%	12.55%	1.047%	2.510%	0.209%	0.502%
Vol (ellipse)	82.22%	197.15%	4.11%	9.86%	0.822%	1.971%	0.164%	0.394%

As this is not a global map, I cannot make assumptions about how our results fit a global representation of Europa's surface. Even if the global map was entirely moderate-resolution Galileo imagery, the uncertainty within individual measurements is significant. There are many possible details which may influence our results. For example, I am assuming that the bands need to propagate through the ice shell into the liquid water ocean, so the depth is equal to the thickness of the ice shell. However, if there were pockets of liquid water within the ice shell, they could serve as a temporary source for some of the observed bands. Pockets

of liquid water could exist through a number of mechanisms mentioned in Section 2, including through the formation of brine pockets through salt water freezing and through thermal plumes which have been hypothesized to create chaos terrain on the surface. This water could potentially source some of the small-scale bands that we observe on the surface, though this theory does not explain the formation of large-scale bands that extend for thousands of kilometers and span tens of thousands of square kilometers. Small pockets in the shell could not provide enough water to source these features, meaning a substantial water source (like a global ocean) would be required for building bands of this scale.

As I have only covered 4.6% of the total surface in this study, our results suggest further investigation is necessary to confirm or disprove our initial hypothesis. Surface area calculations for bands and ridges of each region were within 1 order of magnitude, which is a promising initial indication that our hypothesis is plausible. While our final estimate of shell thickness (100-700 m) is on the thin side, it still fits within published values ([Billings & Kattenhorn \(2005\)](#)), and matches results that have used mechanical models of buoyancy, flexure, or lithostatic stresses to estimate shell thickness (typically >1km). Another promising result came when examining the surface area calculations, as our results are of the same order of magnitude as those those presented in [Kattenhorn & Prockter \(2014\)](#). The next steps for improving this work will be adding more sites to create a more global representation of the surface. While it will not be necessary to map all of the moderate-resolution data available on the global mosaic, adding a few similarly sized ridge-dominated regions would help us better understand the distribution of surface features, and determine whether Site 3 could be an outlier among our data set.

## CHAPTER 6: Error Analysis

---

The dominant source of error came from ridge width measurements, which were only accurate to  $\pm 1$  pixel on each side. With pixel resolution at about 500 m, including an extra pixel on each side of the ridge would result in an error of  $\pm 1$  km. Average ridge width was between 1.2 - 3 km, so the uncertainty corresponds to a maximum error of  $\pm 83.3\%$ . This is a large margin of error, and results in surface area and volume uncertainties of the same order of magnitude as the calculated results. Our measurements are limited in accuracy due to the limited resolution of the Galileo images.

We cannot change the nature of the resolution of this data, so to attempt to make the average shadow length and width as accurate as possible, they were measured approximately once every 10 km. These calculations are based on measurements of one person, so it would strengthen our results to have multiple scientists mapping using the same techniques described in Appendix A. In the future, we should also map more sites at varying locations on the surface, with multiple mappers having measured the same site to compare results.

It is also important to mention the significance of my own biases while mapping. In wanting the measurements to be reproducible, I attempted to stick to a consistent pattern of mapping. However, with the moderate resolution images, the boundaries of ridge widths or shadow lengths can become blurred. As previously mentioned, deviations of just one pixel on either side of the feature during measurements can result in a high magnitude of error. Therefore, it would be interesting in future work to turn this into a citizen scientist project, where several volunteers could map a region given the detailed mapping itinerary, and the results could be analyzed in order to determine the magnitude of these bias-related effects. While this would have strengthened the results of this work, it was deemed unnecessary at this point in our project, though would be a useful inclusion for the continuation of this research.

## CHAPTER 7: Future Missions

---

### 7.1 Europa Clipper

Galileo's mission ended in 2003, and many believe we are long overdue for another mission to the Europa. Recently, NASA and the European Space Agency have proposed missions to return to the Jupiter system. As of March 2019, NASA has requested \$600 million to fund a Europa-exclusive flyby mission, set to launch in June 2023 ([Verma & Margot \(2018\)](#)). The mission has been dubbed the Europa Clipper and will have nine instruments selected to fulfill the following primary objectives:

- (1) To determine the thickness of the ice shell.
- (2) To search for subsurface lakes similar to the subglacial lakes found on Earth.
- (3) To measure magnetic field strength and direction to make calculations of the depth and salinity of the ocean.
- (4) To search for recent thermal eruptions at the surface and further evidence of tectonic processes.
- (5) To confirm the existence of speculated water plumes near the southern pole.
- (6) To take images using a high-resolution camera and spectrometer to study the surface chemistry of Europa.

According to [Verma & Margot \(2018\)](#), Europa Clipper will include cameras paired with spectrometers to capture high-resolution images with associated chemical compositions. As previously expressed, attempts at mapping spectrometer data from Galileo to their corresponding images has proven unsuccessful, so we have not been able to identify the chemical composition of individual surface features. This inclusion will have the potential to solve many unanswered questions, and may provide evidence in favor of different formation mechanisms for bands and ridges presented in Section 2.

Europa Clipper would also carry an ice-penetrating radar to determine the thickness of the ice shell, a value which has eluded scientists for decades, and a major

component of this research. The spacecraft will be able to detect variability in thickness and be able to locate proposed subsurface lakes or lenses between the ice and the liquid water ocean. If this data could also be matched with surface features, we may be able to confirm some theories of chaos terrain or band formation. Several other instruments will measure the magnetic field and gravitational measurements to further probe the subsurface ocean, as well as a thermal measurer to look for hot eruptions near the surface. The mission would take the spacecraft on 45 flybys of Europa with altitudes between 16–1700 miles above the surface.

## 7.2 JUICE

NASA is not the only space organization interested in studying Europa. The JUpiter ICy moons Explorer (JUICE) mission is a European Space Agency (ESA) funded mission, approved in 2012 and set to arrive at the Jupiter system in 2030 (Grasset et al. (2013)). While the main priority of the mission is to study Jupiter and the habitability of Ganymede, the spacecraft will also make flybys of Europa and Callisto. Europa will receive two flybys, which Grasset et al. (2013) claim will have a focus on studying the chemistry of the moon and to look for organic molecules and other possible biosignatures. This mission will provide some of the most high resolution (several m/pixel) of several high-priority targets, as well as topography studies with subsurface mapping from different instrumentation, which will give constraints on the global age of the surface. The spectrometer will allow study of the surface composition, with spectral mapping resolution up to 1 km/pixel. With this data, we may be able to determine the composition of individual geological surface features, including the linear fractures, chaos terrains, craters, ridges and bands. The subsurface radar sounding instrument will be able to penetrate the subsurface to a depth of up to 9 km with a vertical resolution of some tens of meters. In combination with data from Europa Clipper, hopefully JUICE will be able to clear up the controversy surrounding the thickness of ice and depth of the ocean, especially beneath active regions like newly forming chaos terrain where temperature is likely at a local maxima. Finally, this mission will provide the high-resolution images which may reveal potential future landing sites on the surface.

## CHAPTER 8: Conclusion and Future Work

---

In this work we have explored some of the literature surrounding Europa's tectonics, global ocean, orbital mechanics, and the variety of geological features on the surface. Of these many features, bands have been documented as extensional features where new crust is created, and can exist over a wide range of albedos. However, if unaccounted for by another process, band extension would cause the total volume of ice on Europa to increase over time. We began with a hypothesis where compressional ridges may compensate for the volume of ice created through band expansion.

To test this hypothesis, we selected four sites across a global mosaic of Europa which fit my chosen criteria: they include moderate-resolution Galileo coverage to ensure we are using the highest resolution available on the global mosaic, and have solar incidence angles between 20-70° to ensure the site has a contrast which allows us to detect the most surface features. We also selected regions at a variety of longitudes and latitudes in order to achieve a more global representation.

My results for the surface area comparison of ridges and bands are in agreement with values published in the tectonic reconstruction of [Kattenhorn & Prockter \(2014\)](#) and we see that Sites 1, 2 and 4 appear to be band-dominated. Calculations for Site 3 predict a ridge-dominated surface. These are in agreement with global observations of Europa that show a surface divided into ridge-dominated and band-dominated regions. Volume estimates showed that a shell thickness of 100-700 m would allow for ridge compression to accommodate for band extension. While this is thin when compared to published values which are often on the order of several kilometers ([Billings & Kattenhorn \(2005\)](#)), it fits within shell estimates which use mechanical models to predict a shell thickness of <1 km.

The shell thickness estimated range of 100-700 m did not disprove our initial hypothesis, but it was on the low end of even the thinnest predictions for shell thickness (>1km), which makes it appear unlikely that ridges alone could accommodate for the total volume of ice being produced through band extension. Our model does not account for the increased density of ice that would exist at

compressional ridges, and so the ridge volumes would be underestimates of their actual value. Additionally, as discussed in Chapter 2, band extension may not begin where bands meet the ocean, but instead could be sourced by pockets of liquid water trapped in the shell from thermal plumes from the interior. In this case, our band volume would be overestimates. In combination, if our ridge volumes were underestimates and our band volumes were overestimates, then our results might have better agreement with our initial hypothesis. But even if we doubled the total ridge volume to simulate an ice that was compressed, it would still only correspond to a crust thickness around 1 km.

From these volume estimations, I have not been able to definitively prove or disprove our initial hypothesis, though they indicate it is unlikely that ridges alone can compensate for the ice created through band extension. Moving forward, we may alter this hypothesis and reanalyze our mapping results after incorporating more details like those in [Rhoden et al. \(2012\)](#) to make our models less simplistic and more accurate to our current understanding of Europa.

The immediate next steps for this work would be to expand the mapping coverage, starting with including more ridge-dominated regions and comparing them to my results for Site 3. Despite their different total areas, Sites 1, 2 and 4 have comparable ratios of ridge to band surface areas. It would be interesting to see how our results change with the incorporation of more ridge-dominated regions: will they be similar to our results for Site 3, or could Site 3 be an outlier? I could also incorporate some of the complex details that [Rhoden et al. \(2012\)](#) include in their model such as a relaxation factor, crustal warping, and accumulated stresses in the shell.

The prospects are bright for the future of Europa study. This work may be able to build off of data from the Europa Clipper and JUICE missions, which have the capability to reveal precise measurements of the ice-shell thickness, and narrowing down a range of values for this measurement has been a major focus of this work. These missions may also provide important context necessary to confirm or refute past hypothesis of ridge and band formation. In short, these missions will revolutionize our understanding of the moon, but in the until then, European scientists will continue to explore it with whatever means are available.

## APPENDIX A: Mapping Techniques

---

Numbered process to ridge and band mapping in QGIS:

- 1) For the region you want to map, locate the label file from <https://pilot.wr.usgs.gov/>. Make note of the north azimuth, subsolar azimuth, and incidence angle.
- 2) Create a polygon around the region that is identical to the image from the map on the Pilot website. This will act as the boundary for mapping features in this region.
- 3) Create two groups in the layer toolbar called “Bands Site X” and “Ridges Site X” with X being the site number. Create a band polygon layer, band length and band width line layers under “Bands Site X” , and ridge, ridge width, and shadow length line layers under “Ridges Site X”.
- 4) Starting with bands, draw polygons around each band feature in the site. Remember that bands have a high range of albedo, so don’t map based on color alone. Only include areas that you are sure are part of the band features.
- 5) For the band length layer, measure the length of the band along the center of the feature.
- 6) For the band width layer, measure the width along even increments. I used 9-10km increments.
- 7) For ridges, start by measuring the ridge length in the ridge line layer, following the center of the ridge.
- 8) Measure ridge width at equal increments. I used 10km increments for Sites 1-3. Keep in mind that you want to underestimate ridge features, so if you’re not sure where a ridge ends between 2 pixels, choose the one that makes the ridge smaller. Stay consistent with this method throughout ridge mapping.
- 9) Measure shadow length at the same increments used for ridge widths. Take the shadow measurement starting from the center of the ridge. During the data analysis phase, you’ll subtract  $\frac{1}{2}(\text{width})$  from this value to get a more accurate shadow length. To find the shadow angle, take the subsolar azimuth – north azimuth from the label files: this will be the shadow angle from north. Sometimes you will have to apply a correction factor of  $90 - (\text{subsolar azimuth} - \text{north azimuth})$  before the shadow is in the correct orientation. To check, use the angle tool and find a

crater or a short ridge in the region to see if the original angle makes sense. If it seems offset by  $90^\circ$ , apply the correction factor. If there is no measurable shadow directly at that increment, use one that's slightly offset. It's better to have some data than none. If there is no measurable shadow between 2 increments, skip this measurement and move onto the next one.

10) Once you've completed all these measurements, move on to calculations. The formulas used in the calculations are given in Section 3. Note that the incidence angle given in the label file is measured from the ground to the sun, so to make it work using the calculation in Section 3.3.2, take  $90 - (\text{incidence angle})$  and use this value as the incidence angle for the site. I used an Excel spreadsheet to make these calculations, but any data analysis program/tool will suffice.

## Bibliography

- Bierhaus, E., Chapman, C., & Merline, W. 2005, *Nature*, 437, 1125
- Billings, S., & Kattenhorn, S. 2005, *Icarus*, 177, 397
- Gaidos, E., & Nimmo, F. 2000, *Nature*, 405, 637
- Geissler, P., Greenberg, R., Hoppa, G., et al. 1998, *Icarus*, 135, 107
- Grasset, O., Dougherty, M. K., Coustenis, A., et al. 2013, *Planet. Space Sci.*, 78, 1
- Greeley, R., Sullivan, R., Klemaszewski, J., et al. 1998, *ICARUS*, 135, 4
- Greeley, R., Figueredo, P., Williams, D., et al. 2000, *Journal of Geophysical Research*, 105, 2559
- Greenberg, R., Geissler, P., Hoppa, G., et al. 1998, *Icarus*, 135, 64
- Hall, D., Strobel, D., Feldman, P., McGrath, M., & Weaver, H. 1995, *Nature*, 373, 677
- Head, J. W., Pappalardo, R. T., & Sullivan, R. 1999, *Journal of Geophysical Research: Planets*, 104, 24223
- Hoppa, G., Tufts, B., Greenberg, R., & Geissler, P. 1999, *Science (New York, N.Y.)*, 285, 1899
- Jia, X., Kivelson, M. G., Khurana, K. K., & Kurth, W. S. 2018, *Nature Astronomy*, 2, 459
- Johnston, S., & Montesi, L. 2014, *Icarus*, 237, 190–201
- Kargel, J. S., Kaye, J. Z., Head, J. W., et al. 2000, *Icarus*, 148, 226
- Kattenhorn, S. 2004, *Icarus*, 172, 582
- Kattenhorn, S., & Prockter, L. 2014, *Nature Geoscience*, 7, 762
- Kivelson, M., Khurana, K., Stevenson, D., et al. 1999, *Journal of Geophysical Research*, 104, 4609

- Klaser, M., Gross, J., Tindall, S., Schliche, R., & Potter, C. 2018, *Icarus*, 321, doi:10.1016/j.icarus.2018.11.005
- Leonard, E. J., Pappalardo, R. T., & Yin, A. 2018, *Icarus*, 312, 100
- Müller, R. D., Sdrolias, M., Gaina, C., & Roest, W. R. 2008, *Geochemistry, Geophysics, Geosystems*, 9, doi:10.1029/2007GC001743
- Ogihara, M., & Ida, S. 2012, *The Astrophysical Journal*, 753, doi:10.1088/0004-637X/753/1/60
- Pappalardo, R. 2010, *Proceedings of the International Astronomical Union*, 6, 101
- Pappalardo, R., Belton, M., Breneman, H., et al. 1999, *Journal of Geophysical Research*, 104, 24,015
- Pappalardo, R., Vance, S., Bagenal, F., et al. 2013, *Astrobiology*, 13, doi:10.1089/ast.2013.1003
- Pasek, M. A., & Greenberg, R. 2012, *Astrobiology*, 12, 151
- Peale, S. J., & Lee, M. H. 2002, *Science*, 298, 593
- Podolskiy, E. A., & Walter, F. 2016, *Reviews of Geophysics*, 54, 708
- Prockter, L., Head, J., Pappalardo, R., et al. 2002, *Journal of Geophysical Research*, 107, 4
- Quick, L. C., & Marsh, B. D. 2016, *Journal of Volcanology and Geothermal Research*, 319, 66
- Rhoden, A., Wurman, G., Manga, M., & Hurford, T. 2012, *Icarus*, 218, doi:10.1016/j.icarus.2011.12.015
- Roth, L., Saur, J., Retherford, K., et al. 2013, *Science (New York, N.Y.)*, 343, doi:10.1126/science.1247051
- Schmidt, B., Blankenship, D., Patterson, G., & Schenk, P. 2011, *Nature*, 479, 502
- Showman, A. P., & Malhotra, R. 1999, *Science*, 296, 77
- Stempel, M. M., Barr, A. C., & Pappalardo, R. T. 2005, *Icarus*, 177, 297

*Bibliography*

61

Sullivan, R., Greeley, R., Homan, K., et al. 1998, *Nature*, 391, 371

Verma, A. K., & Margot, J.-L. 2018, *Icarus*, 314, 35